8 Generation and Measurement of Structure-Borne Sound

8.1 Mechanical Measurement Methods

8.1.1 Registration of Motion

Most "structure-borne sound sensors" respond to kinematic variables such as displacement, velocity or acceleration. Dynamic quantities such as stresses are usually deduced from differences of the former. The reason for this is in part that the kinematic variables are normally simpler to register than tensor quantities like stresses and strains despite their directional dependencies. Moreover, usually only the exterior of some structure-borne sound field is accessible for measurements whereas the field is disturbed if the structure is penetrated to reach interior points.

The measurement technique that is simplest to visualize consists of direct observation of the excursion i.e., of the displacement of the test object relative some fixed body, supporting a scale, as sketched in Fig. 8.1. Because these excursions generally are very small, only some enlarged or amplified observation can be made. Such a direct observation therefore is limited largely to calibration instruments in the laboratory.

Optical amplification of excursions from an equilibrium position can be primitively obtained by means of a mirror deflecting a light beam. If one

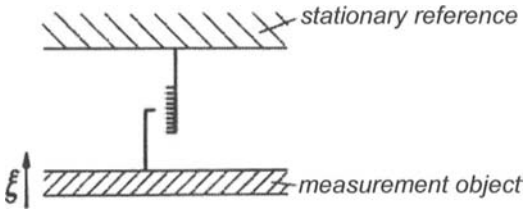

Fig. 8.1. Arrangement for direct observation of test object displacement

edge of a mirror of length l is displaced by an amount ξ, while the other edge pivots about a fix axis as depicted in Fig. 8.2, the mirror rotates an angle ξ/l. An impinging light beam accordingly is deflected twice that angle and a spot of the light, reflected at a screen at a distance L, is displaced by

$$\Delta = \xi\,(2L/l), \tag{8.1}$$

relative the equilibrium reflection point. Since an amplification of $2L/l = 500$ can be readily achieved, a test object displacement of 0.01mm not only can be measured but also the time history can be registered.

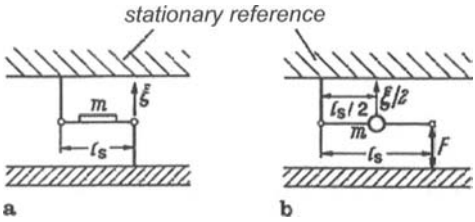

Fig. 8.2. Observation of displacement by means of a pivoted mirror. a) mirror attached to a lever and b) mass lever substitution

The rotating mirror sensor differs in one important aspect from the direct observation. Whereas a direct observation leads to no reaction force on the test object, the mirror inertia results in a force

$$\underline{F} = -\frac{1}{l}\left(\frac{\omega^2 m}{2}\frac{l}{2}\right)\underline{\xi} = -\frac{\omega^2 m}{4}\underline{\xi}\,. \tag{8.2}$$

A similar relation applies to any instrument, with which a displacement is to be registered by means of a system of levers.

Because the reaction force produced by the sensor varies with frequency squared for a given displacement, such tilting mirrors and mechanical lever systems clearly are useful only for low frequencies. This limitation, also, becomes apparent if one notes that as for airborne sound, the square of the particle velocity but not the square of the displacement is proportional to the energy in the structure-borne sound context. Thus, for given energy, the displacement is inversely proportional to frequency. The dynamic variables force and strains associated with propagating waves, also, are proportional to the particle velocities and the products of forces and

portional to the particle velocities and the products of forces and velocities constitute the corresponding power quantities.

The most appropriate way to assess the reaction of a vibration sensor on a measurement object is to compare the mobility of the sensor $\underline{Y}_a$ with that of the object $\underline{Y}$ at the point of measurement. The latter mobility determines the velocity of the object induced by the force. This velocity alters the velocity of the unloaded object from the initial v_0 to

$$\underline{v} = \underline{v}_0 - \underline{Y}\,\underline{F} = \underline{v}_0 - \left(\underline{Y}/\underline{Y}_a\right)\underline{v}\,. \tag{8.3}$$

The relative difference between the velocity sought v_0 and the actually measured velocity v, therefore, obeys

$$\left(\underline{v}_0 - \underline{v}\right)/\underline{v} = \underline{Y}/\underline{Y}_a\,. \tag{8.3a}$$

For the previously described pivoted mirror, the sensor mobility is given by

$$\underline{Y}_a = 4/\left(j\omega\, m\right), \tag{8.4}$$

which thus is proportional to frequency. The factor $-j$ indicates that the velocity lags the force by a phase angle of $\pi/2$.

8.1.2 Comparison with Known Mobilities

If the sensing edge of the pivoted mirror of the previous section is kept in contact with the object only by gravity and the vibration of interest is in the vertical direction, the mirror cannot follow downward accelerations that exceed the acceleration of gravity. The force exerted by the object on the edge of the mirror cannot be negative,

$$F = m(g + \ddot{\xi}) > 0\,. \tag{8.5}$$

This '1g' acceleration threshold is useful for absolute calibration of vibration sources such as shakers and vibration tables. Moreover, different thresholds can be achieved by using preloaded springs to force a known mass against the vibrating object as depicted in Fig. 8.3. Such a device also applies in the case of horizontal motion. In the vertical case, the force, which again cannot become negative, obeys

$$F = F_s + m(g + \ddot{\xi}) + s\xi > 0\,, \tag{8.6}$$

where s denotes the spring stiffness. By considering harmonic motion and introducing the natural frequency $\omega_0 = \sqrt{s/m}$, the displacement amplitude is found from Eq. (8.6) to be given by

$$\hat{\xi} = \frac{F_s/m + g}{\omega^2 - \omega_0^2}. \tag{8.7}$$

A mass that is pressed by a prestressed spring against a measurement object, thus, can serve as an acceleration sensor only if the excitation frequency is substantially larger than the natural frequency of the mass-spring system. Accordingly, the mass cannot be too small and the spring cannot be too stiff. In spite of these limitations, early measurements were successfully carried out on membranes [8.1].

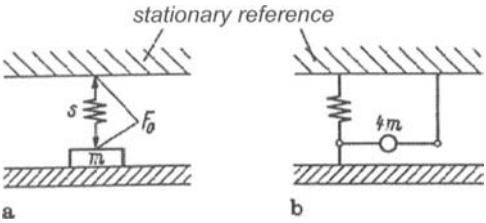

Fig. 8.3. Spring-loaded mass used as an acceleration threshold indicator. a) mechanical configuration and b) mechanical 'circuit' using a mass lever

At resonance i.e., when the excitation frequency coincides with the natural frequency of the sensor, the displacement amplitude tends to infinity. This condition, however, does not result in a particularly large reaction force on the measured object. Rather, the oppositely phased spring and inertia forces, making up the force F acting on the sensor

$$\underline{F} = \left(j\omega m + \frac{s}{j\omega} \right) \underline{v}, \tag{8.8}$$

cancel each other. This means that the sensor mobility tends to infinity at this frequency.

From Fig. 8.3, it would be tempting to term the mass and spring connected in series. Such a description must not be confused with a series connection in an electrical sense. Clearly, the same force as given by (8.8) also results when the mass and spring are attached side by side to the vibrating object. The lower and upper side of the mass in Fig. 1.4a, moreover, do not correspond to the "input" and "output" of an electrical two-pole. Rather, the force here is exerted at the same pole of the mass, with the opposite pole being the inertial reference for the acceleration.

The topology of the mechanical system can readily be translated to an electrical circuit when the mass is replaced by a mass lever [8.2] with a point mass at its midpoint, as depicted in Fig. 1.4b. From the considerations of the pivoted mirror, the point mass must be $4m$ to result in an inertia force of $j\omega m$. Accordingly, the "mechanical circuit" in Fig. 1.4b much better displays the physics of the mass and spring being connected in parallel. This is also in accordance with the electrical analogy where the branching forces correspond to the branching currents. The force "flow" in the mass lever, however, differs in one respect from the current in a branch of an electrical circuit. Although the force has the same magnitude before and after the mass, its algebraic sign is reversed. This effect is important if the other pivot rests on a mobile body instead of being fixed in space such that the mass lever acts as a coupling element. The sign of the force may be reversed once more by replacing the single mass lever by two such levers, mechanically in series.

The fact that a mechanical series connection provides no information regarding the topology of the analogous electrical circuit is also illustrated by the observation that the mobility is fully altered when the configuration shown in Fig. 8.4a is considered instead of the previously discussed sensor design of Fig. 8.3a. Here, the spring is situated between the vibrating object and the mass. In this arrangement no branching force occurs but the force at the "input" flows unperturbed through the spring to the mass. In contrast, the displacement of the mass differs from the compression of the spring. This difference becomes very clear when the two "mechanical circuits" in Figs. 8.3b and 8.4b, employing mass levers, are compared.

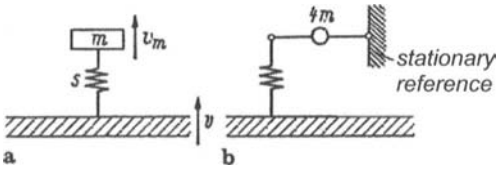

Fig. 8.4. Simple oscillator representing a sensor. a) mechanical system and b) mechanical circuit

By adding the two relations

$$\underline{v}_m = \underline{F}/(j\omega m) \quad , \quad \underline{v} - \underline{v}_m = j\omega \underline{F}/s \tag{8.9}$$

the mobility can be established of the sensor at the contact point with the object,

$$\underline{Y} = \left(\frac{j\omega}{s} + \frac{1}{j\omega m} \right), \tag{8.10}$$

which vanishes at the mass-spring resonance. The velocity of the mass, on the other hand, tends to infinity for a given velocity of the object, as seen from the relation

$$\underline{v}_m = \frac{\underline{v}}{1 - \left(\omega/\omega_0\right)^2}, \tag{8.11}$$

also obtained from (8.9). This result indicates that small motions, invisible to the naked eye, in principle, can be enlarged by resonant systems and not only by microscopes and optical levers.

8.1.3 Mechanical Transducers as Damped Mass-Spring Systems

The mechanical systems considered in the previous section must be augmented by the inevitable dissipation to realistically represent transducers for structure-borne sound. As discussed in Chapter 4, many different types of dissipation exist but only the most simple, namely the viscous element, will be considered in this context, realizing a force proportional to the velocity

$$F_r = -rv. \tag{8.12}$$

Herein, r is the viscous damping coefficient, which depends on the shape of the moving body and the ambient fluid. As introduced in Fig. 8.5, the viscous element is represented by a symbol that should associate to a piston in a cylinder, a "dash-pot". Again, the viscous element acts physically in parallel with the mass, as is evident from the mechanical circuit in Fig. 8.5b.

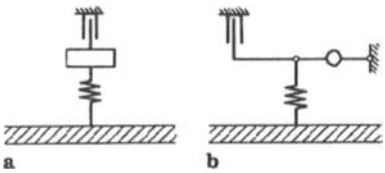

Fig. 8.5. Simple oscillator with linear frictional resistance. a) mechanical system and b) mechanical circuit

The input mobility of the sensor can be found to be given by

$$\underline{Y} = \frac{1-\left(\omega/\omega_0\right)^2 + j\omega r/s}{j\omega m + r}, \tag{8.13}$$

which does not vanish at resonance. Instead, it takes on the real value

$$\underline{Y}_0 = \frac{r}{sm} \tag{8.14}$$

at the resonance for small enough damping coefficients, satisfying the inequality $r << \omega_0 m$. The mobility, therefore, is the larger the smaller the mass and spring stiffness and the larger the damping coefficient.

The transmissibility $\underline{v}_m/\underline{v}$ can be derived as

$$\frac{\underline{v}_m}{\underline{v}} = \frac{1}{1-\left(\omega/\omega_0\right)^2 + \dfrac{j\omega r}{s}}, \tag{8.15a}$$

which has the magnitude squared

$$\left|\frac{\underline{v}_m}{\underline{v}}\right|^2 = \frac{sm}{r^2} \tag{8.15b}$$

at resonance. In principle, it thus appears possible to observe the displacement ξ_m, corresponding to v_m, from which the displacement of the test object ξ can be determined. This measurement method is not practical, however, not only because the dissipation usually is due to mechanisms other than pure viscous damping and is difficult to assess but foremost because the resonance peak is very narrow.

In order to describe the resonance peak in more general form, Eq. (8.15a) can be rewritten in terms of the decay constant, characterizing the decay of free oscillations

$$\xi = \hat{\xi} e^{-\delta t} \cos(\omega t + \varphi_\xi) = \mathrm{Re}\left[\underline{\hat{\xi}} e^{-(\delta + j\omega)t}\right] \tag{8.16}$$

of the system depicted in Fig. 8.5 with the oscillating object held fix. By introducing (8.16) in the equation of motion

$$m\ddot{\xi} + r\dot{\xi} + s\xi = 0, \tag{8.17}$$

one finds that the decay constant is related to the damping coefficient as

$$\delta = \frac{r}{2m} \tag{8.18a}$$

and that the eigen-frequency reduces to

$$\omega = \sqrt{\omega_0^2 - \delta^2} \tag{8.18b}$$

The transmissibility, which can be rewritten as

$$\frac{\underline{v}_m}{\underline{v}} = \frac{1}{1-\left(\omega/\omega_0\right)^2 + j\omega\dfrac{2\delta}{\omega_0^2}}, \tag{8.19}$$

is shown in Fig. 8.6 for a damping ratio of $r/r_c = \delta/\omega_0 = 0.1$ where $r_c = 2\sqrt{sm}$ is the critical damping. The graph does not exhibit a pole but a pronounced peak at the damped eigen-frequency. By differentiating the square of the denominator magnitude with respect to ω^2, the peak frequency can be found to obey

$$\omega = \sqrt{\omega_0^2 - 2\delta^2} \approx \omega_0(1-\delta^2/\omega_0^2)\,. \tag{8.20}$$

For small enough damping ratios, the difference between the undamped and the damped eigen-frequency can be neglected such that $\omega \approx \omega_0$ and the magnitude follows

$$v_{m,\max} \approx \frac{\omega_0}{2\delta} v \tag{8.21}$$

in the vicinity of the peak.

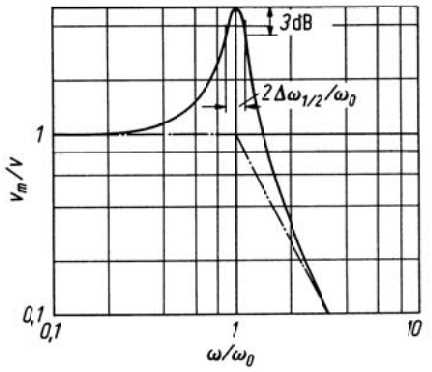

Fig. 8.6. Motion transmissibility of the simple oscillator in Fig. 8.5

With the frequency deviation $\Delta\omega = \omega - \omega_0$ introduced and neglecting terms of the order $(\Delta\omega)^2$, the ratio of oscillator velocity to maximum velocity

$$\frac{\underline{v}_m}{\underline{v}_{m,\max}} = \frac{1}{1 + j\Delta\omega/\delta} \tag{8.22a}$$

is obtained. Such a relation between a field variable and its maximum resonance value as function of the frequency deviation can be viewed as a definition of the "resonance function". This function not only describes the parabolic region in the vicinity of the peak

$$\left|\frac{\underline{v}_m}{\underline{v}_{m,\max}}\right| \approx 1 - \frac{1}{2}\left(\frac{\Delta\omega}{\delta}\right)^2, \tag{8.22b}$$

but is valid also below the inflection points for small enough δ. The function thus describes the "bell-shaped" amplitude curve versus frequency deviation, which is common for all resonance phenomena. On a logarithmic scale, the inflection points occur where the magnitude squared and thus the power is half of the peak value. The corresponding frequency deviation is found from Eq. (8.22) to be

$$\Delta\omega_{1/2} = \delta \ . \tag{8.23a}$$

Twice this deviation can be considered a reasonable measure of the width of the resonance peak and is termed the half-value or half-power bandwidth. This bandwidth is usually given in Hz such that

$$2\Delta f_{1/2} = \delta/\pi \tag{8.23b}$$

Measured from the amplitude, the bandwidth is obtained at $1/\sqrt{2}$ of the maximum amplitude.

In order to obtain large peak velocities, small damping coefficients, decay constants or damping ratios are required. The small damping means, however, that the half-value bandwidth is limited. The associated strong variation with frequency of the response of lightly damped systems near their resonances makes them unsuitable as structure-borne sound sensors.

On the other hand, lightly damped mechanical systems are well suited for use as frequency indicators. In this respect, mechanical systems are usually better than electrical because their damping can be made much smaller.

8.1.4 Interaction of Transducer and Measurement Object

Any measurement implies that the object or its behaviour is affected, albeit ever so little. Since this general law naturally applies also for structure-borne sound measurements and the effect is not always evident, the issue will be analysed in this section through some examples.

The first situation considered is outlined in Fig. 8.7. It involves an oscillator attached to a vibrating object with a prescribed velocity $\underline{v}$. The oscillator mass m_M is connected to the object via springs of total stiffness s_M. On top of the oscillator, a transducer of mass m is attached via some spring-like fixture of stiffness s.

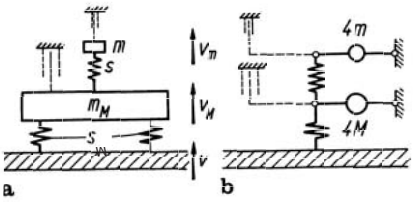

Fig. 8.7. Simple transducer model on top of a simple oscillator. a) mechanical configuration and b) mechanical circuit

For pure harmonic processes of frequency ω, the spring forces are given by

$$\underline{F}_{s_M} = \frac{s_M}{j\omega}(\underline{v} - \underline{v}_M),\ \ \underline{F}_s = \frac{s}{j\omega}(\underline{v}_M - \underline{v}_m)\,, \tag{8.24}$$

for the lower and upper masses respectively. The inertia forces of the masses are obtained from the accelerations $j\omega\underline{v}_M$ and $j\omega\underline{v}_m$ respectively as $\underline{F}_M = j\omega m_M\,\underline{v}_M$ and $\underline{F}_m = j\omega m_m\,\underline{v}_m$. The force balances require

$$\underline{F}_M = \underline{F}_{s_M} - \underline{F}_s \ \Rightarrow\ \frac{s_M}{j\omega}(\underline{v} - \underline{v}_M) - \frac{s}{j\omega}(\underline{v}_M - \underline{v}_m) = j\omega m_M\,\underline{v}_M \tag{8.25a}$$

and

$$\underline{F}_m = \underline{F}_s \ \Rightarrow\ \frac{s}{j\omega}(\underline{v}_M - \underline{v}_m) = j\omega m\underline{v}_m\,. \tag{8.25b}$$

This yields the coupled system of equations

$$\begin{aligned}(-\omega^2 m_M + s_M + s)\underline{v}_M - s\underline{v}_m &= s_M \underline{v},\\ -s\underline{v}_M + (-\omega^2 m + s)\underline{v}_m &= 0,\end{aligned} \tag{8.26}$$

from which the transmissibilities

$$\frac{\underline{v}_M}{\underline{v}} = \frac{1-(\omega/\omega_0)^2}{\left(1+\frac{s}{s_M}-\frac{\omega^2}{\omega_M^2}\right)\left(1-\frac{\omega^2}{\omega_m^2}\right)-\frac{s}{s_M}}, \tag{8.27a}$$

and

$$\frac{\underline{v}_m}{\underline{v}} = \frac{1}{\left(1+\frac{s}{s_M}-\frac{\omega^2}{\omega_M^2}\right)\left(1-\frac{\omega^2}{\omega_m^2}\right)-\frac{s}{s_M}} \tag{8.27b}$$

are obtained. Herein, $\omega_m = \sqrt{s/m}$ and $\omega_M = \sqrt{s_M/m_M}$ are the eigenfrequencies of the separated mass-spring systems.

Equation (8.27a) shows that the presence of the small mass m considerably affects the motion of the oscillator mass m_M at certain frequencies:

- At the zeroes of the denominator i.e., for frequencies above ω_m and below ω_M respectively provided $\omega_m < \omega_M$, resonances appear

$$\omega_{I,II}^2 = \frac{1}{2}\left[\omega_m^2 + \omega_M^2 + \frac{s}{m_M} \pm \sqrt{\left(\omega_m^2 + \omega_M^2 + \frac{s}{m_M}\right)^2 - 4\omega_m^2\omega_M^2}\right], \tag{8.28}$$

  which would not occur in the absence of the transducer mass m.
- At the frequency $\omega = \omega_m$, the mass m_M is completely stopped i.e., an antiresonance occurs and $\underline{v}_M = 0$. In the special case of $s_M/m_M = s/m$ such that $\omega_M = \omega_m$, the biggest alteration is introduced, namely a transition from an infinitely large to a vanishingly small velocity since the resonance frequency ω_M, would equal ω_m in the absence of the transducer mass m.

Although the effects mentioned above still occur when dissipation is taken into account, they are not so pronounced. The corresponding analysis for the system sketched in Fig. 8.7 with the dashpot included, fixed to some inertial frame, simply means that the viscous forces are added on the right-hand side of Eqs. (8.25). Such a modelling to some extent, would represent the friction associated with the motion of the masses in the ambient medium. In a case where the dissipation is associated essentially with material losses in the springs, the dashpots must be re-arranged parallel to

the former. This would mean that $s/j\omega$ in Eq. (8.25) would be replaced by $r + s/j\omega$ and $s_M/j\omega$ by $r_M + s_M/j\omega$.

Figure 8.8 shows the transmissibility $\underline{v}_M/\underline{v}$ as function of frequency, with and without the transducer. In the example is assumed equal eigenfrequencies for the two cascaded oscillators i.e., $s_M/m_M = s/m$ and $r_M/m_M = r/m$. The small mass and the damping ratio, moreover, are set to be $m = m_M/10$ and $\delta/\omega_0 = r/2\ sm = 0.1$. Strong interaction is clearly seen in the vicinity of the resonance whereas the effect is negligible elsewhere for small ratios m/m_M.

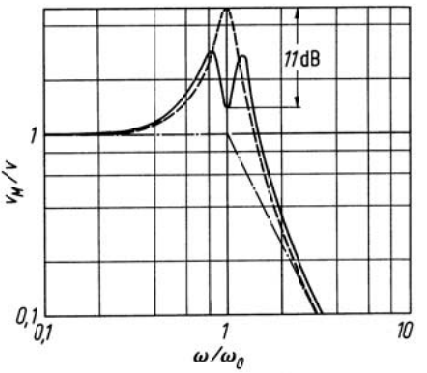

Fig. 8.8. Motion transmissibility of the simple oscillator. (——) with and (- - -) without a tuned transducer

All the drawbacks associated with resonance phenomena of a tuned transducer could be ameliorated by making the damping ratio so large that no or only little resonant amplification would arise. Such a damping is difficult to achieve, however, for the relatively large masses of structure-borne sound transducers. In practice, therefore, tuned transducers are only designed with their resonances either well above or well below the frequency range of interest.

The mechanical system depicted in Fig. 8.7 not only is of great significance for structure-borne sound measurement techniques. It is also a model for the so-called dynamic absorber i.e., small mass-spring systems, which are mounted on resonantly vibrating structures, in this case a large mass. As is observed, the resonance amplitude can be reduced substantially already with a relatively small dynamic absorber.

As a second example, Fig. 8.9 presents an idealization of a useful structure-borne sound exciter. It consists of a small coil mass m_1, which is connected to the test object by means of a stiff spring s_1, for example, representing some adhesive. The coil, moreover, is connected via some soft spring s_2 to centre the magnet mass m_2, which, in turn, resiliently rests on the test object on soft springs s_0.

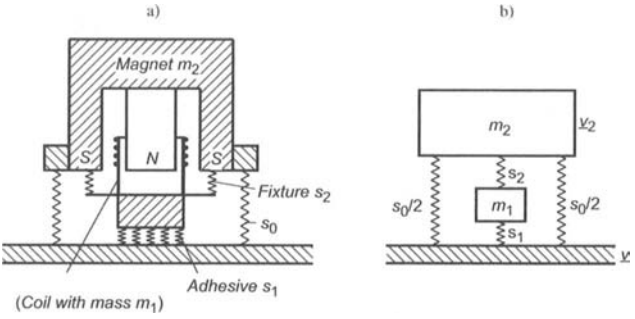

Fig. 8.9. Mechanical configuration of an electro-dynamic exciter. a) principal construction and b) model

Upon temporarily disregarding the electro-dynamic interaction, the system of equations corresponding to (8.26) is obtained from the force balances

$$\begin{aligned} s_0(\underline{v}-\underline{v}_2)+s_2(\underline{v}_1-\underline{v}_2) &= -\omega^2 m_2 \underline{v}_2, \\ s_1(\underline{v}-\underline{v}_1)+s_2(\underline{v}_1-\underline{v}_2) &= -\omega^2 m_1 \underline{v}_1. \end{aligned} \tag{8.29}$$

Solving for $\underline{v}_1$ and $\underline{v}_2$ brings no difficulties and after some manipulation one finds, for example, the relative difference between the test object velocity and that of the coil as

$$\frac{\underline{v}-\underline{v}_1}{\underline{v}} = \frac{\nu^2(\nu^2\mu-\mu-\sigma_2)}{\nu^4\mu-\nu^2(\mu+\sigma_1+\sigma_2)+\sigma_1+\sigma_2-\sigma_2^2}. \tag{8.29a}$$

In this expression are used the abbreviations

$$\mu=\frac{m_1}{m_2},\ \sigma_1=\frac{s_1}{s_0+s_2},\ \sigma_2=\frac{s_2}{s_0+s_2},\ \nu^2=\frac{\omega^2}{\omega_2^2}=\frac{\omega^2 m_2}{s_0+s_2}.$$

From an interaction point of view, the mobility of the exciter, as seen from the test object, is more interesting. This is obtained as

$$\underline{Y}_{exc} = \frac{\underline{v}}{\underline{F}} = \frac{\underline{v}}{\underline{F}_0 + \underline{F}_1}, \tag{8.30}$$

where $\underline{F}$ means the total force exerted, composed of the two spring forces $\underline{F}_0 = s_0\ (\underline{v} - \underline{v}_2)/j\omega$ and $\underline{F}_1 = s_1\ (\underline{v} - \underline{v}_1)/j\omega$. By carrying out the simple but tedious algebra, it is found that

$$\underline{Y}_{exc}\omega m_2 = j\frac{\nu^4\mu - \nu^2(\mu + \sigma_1 + \sigma_2) + \sigma_1 + \sigma_2 - \sigma_2^2}{\nu^2\mu(1 + \sigma_1 - \sigma_2) - (1 + \mu)(\sigma_1 + \sigma_2 - \sigma_2^2)}, \tag{8.30a}$$

where the same abbreviations are used as in Eq. (8.29a).

The magnitude of the exciter mobility, normalized with respect to the mass mobility of the backing magnet, is plotted in Fig. 8.10 for a specific design. For the computations, some small amount of damping is included, which limits the resonance and antiresonances. As expected, the mobility equals the mass mobility of the magnet at low frequencies ($\nu < 1$). In an intermediate range, the exciter mobility essentially is that of the light-weight coil mass but increases rapidly at frequencies there above. The latter range, however, is of little interest from a transducer point of view since the coil is dynamically decoupled and therefore has a significantly smaller amplitude than the test object.

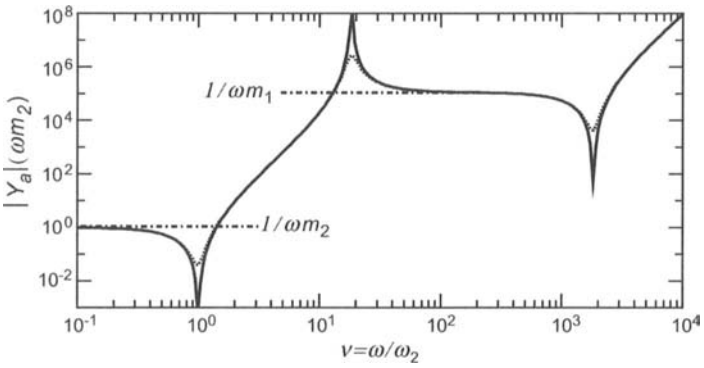

Fig. 8.10. Normalized input mobility of the structure-borne sound exciter in Fig. 8.9. Calculated from Eq. (8.30a) with $\mu = 0.003$, $\sigma_1 = 10000$, $\sigma_1 = 0.95$. (------) loss factor $\eta = 0.01$, (· · · ·) loss factor $\eta = 0.1$, (-·-·-) mass mobility of m_1 and0 m_2

The idealized design is outlined in Fig. 8.11 of another transducer of great practical value. It concerns the mechanical configuration of piezo-electric transducers where the piezo-electric material constitutes the spring

s. Since the electrical charge is proportional to the acting force $\underline{F}_1 = s\,(\underline{v} - \underline{v}_2)/j\omega$, the velocities must be known of the seismic mass m_2 and of the house m_1.

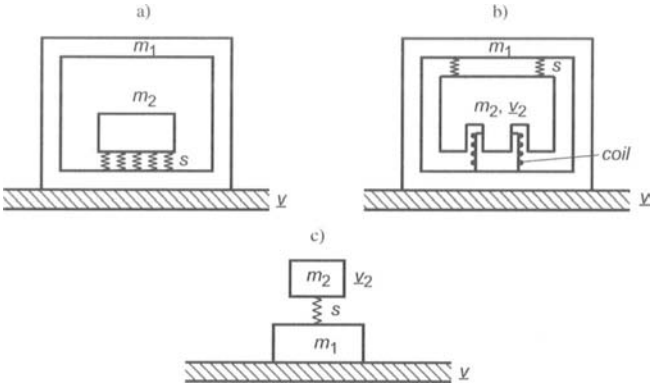

Fig. 8.11. Encapsulated structure-borne sound transducers with "seismic" masses m_2. a) piezoelectric transducer, b) geophone and c) model

For the so-called geophone in Fig. 8.11b, m_2 represents the mass of a magnet with a coil fitted in the air gap. The coil is rigidly connected with the house whereas the magnet is suspended in the soft springs of stiffness *s*. With the voltage proportional to the velocity difference $\underline{v} - \underline{v}_2$, the latter must be determined.

The starting point for the continued analysis, again, is a force balance, which reads

$$s(\underline{v} - \underline{v}_2)/j\omega = j\omega m_2 \underline{v}_2 .$$

From this, both the velocity ratio $\underline{v}_2/\underline{v}$ and the velocity difference in the magnetic field can readily be developed,

$$(\underline{v} - \underline{v}_2) = \underline{v}\frac{1}{1-(\omega_2/\omega)^2} . \qquad (8.31a)$$

For the piezo-electric spring, similarly, the acting force is

$$\underline{F}_1 = j\omega m_2 \underline{v}\frac{1}{1-(\omega/\omega_2)^2} , \qquad (8.31b)$$

where, in both the above expressions, $\omega_2^2 = s/m_2$.

As can be seen, the velocity difference registered by the magnetic transducer approximates well the velocity of the test object for $\omega >> \omega_2$. Accordingly, the geophone is tuned as low frequent as possible to obtain a voltage proportional to the velocity. This means that the spring s is made very soft and the mass m_2 as big as is admissible in view of its mobility.

Contrary, the force $\underline{F}_1$ proves proportional to the acceleration $j\omega\underline{v}$ of the test object in the range $\omega << \omega_2$ and a high frequency tuning is pursued for the piezo-electric transducer.

Finally also, the input mobility of the transducer design is of importance. It is composed of the mass mobility of the house and the reaction from the seismic mass such that

$$\underline{Y}_{transd} = \frac{\underline{v}}{\underline{F}} = \frac{1}{j\omega m_1 + \dfrac{1}{j\omega m_2} + \dfrac{j\omega}{s}} = \frac{1}{j\omega m_1 + \dfrac{j\omega m_2}{1-(\omega/\omega_2)^2}}. \tag{8.32}$$

The last part of (8.32) shows that the mobility vanishes for $\omega^2 = s/m_2$ i.e., the transducer exhibits an antiresonance whereas it tends to infinity and a mass-spring-mass resonance occurs at

$$\omega_{12}^2 = s\left(\frac{1}{m_1} + \frac{1}{m_2}\right).$$

By means of the input mobility of a transducer, its interaction with the test object can be treated in a general way. To see this is considered the situation outlined in Fig. 8.12, where the undisturbed test object exhibits the velocity $\underline{v}_0$ and mobility $\underline{Y}_0$ at the measurement position. Due to the loading from the transducer, the test object's velocity changes from $\underline{v}_0$ to v_m since the transducer reacts with the force $\underline{F} = \underline{v}_m/\underline{Y}_{transd}$. This means that

$$\underline{v}_m = \underline{v}_0 - \underline{F}\underline{Y}_0 = \underline{v}_0 - \frac{\underline{Y}_0}{\underline{Y}_{transd}}\underline{v}_m \Leftrightarrow \underline{v}_m = \underline{v}_0 \frac{1}{1 + \underline{Y}_0/\underline{Y}_{transd}}. \tag{8.33}$$

As is observed, an as unperturbed measurement as possible is obtained for $|\underline{Y}_{transd}| >> |\underline{Y}_0|$. Structure-borne measurement devices, therefore, should be as small and light-weight as possible or as weakly coupled dynamically to the test object as possible. Also, internal transducer resonances should be avoided since they may lead to low mobilities at certain frequencies, which can be difficult to predict. The inevitable interaction mainly leads to a reduction of the vibration velocity. For $|\underline{Y}_{transd}| \approx |\underline{Y}_0|$, however, also an increase is possible since the two mobilities can have opposite signs.

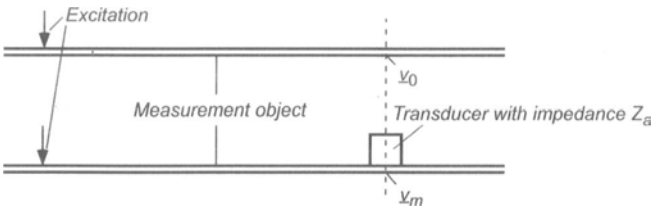

Fig. 8.12. Influence of the transducer mobility on the motion of a measurement object. Only one component of motion is considered

It should be noted that the quantities in Eq. (8.33) usually are complex, which means that the interaction also yields some phase distortion. When such phase errors must be kept small, for instance in conjunction with intensity measurements, the requirements on the condition $|\underline{Y}_{transd}| >> |\underline{Y}_0|$ becomes much more rigorous than for ordinary magnitude or amplitude based measurements.

8.1.5 Immobile Reference and Rigid Termination

For the structure-borne sound transducers illustrated in Figs. 8.1 and 8.2 as well as for numerous other optical and electrical sensors, an "immobile" reference is required. Naturally, this is an ideal condition, which is hardly realizable for frequencies above some hundred Hz since immobile means an absolute motion less than 10^{-6}m or even 10^{-10}m.

A similar, principally unsolvable, problem is the "rigid termination", which is desirable for some structure-borne sound measurement techniques, for example, in conjunction with stiffness measurements. Also in this case an ideal condition is sought that becomes the more insuperable the higher the frequency.

A way out of this dilemma is offered by transducers built according to the mass-spring-mass design cf., Sect. 4.4.1.2 or employing a seismic mass as a reference, as in Fig. 8.11. The basic idea is to replace the unfeasible immobile reference with an element for which the motion can be predicted precisely and thence can be used as the reference. Obviously, not only seismic masses are suitable for this purpose but also any configuration with a known mobility for the component of motion considered.

8.2 Controllable Sensors

For all types of measurements, particularly of oscillatory quantities, it is usually useful to convert any non-electrical quantity to an electrical current or a voltage change. This is so since use can then be made of the entire signal conditioning and processing capabilities provided by modern electronics. For example, the signals can be amplified, filtered, recorded and displayed in many ways and, above all, fed to computers for post-processing and, eventually, the manipulated signals can react on the test object.

Structure-borne sound transducers that convert mechanical quantities to proportional electrical ones may be divided into two groups. For the first, under consideration in this section, the motion of some mechanical element acts on an electrical or optical source without any reaction, except for such small effects as the radiation pressure or the local rise in temperature. The transduction phenomena on which such sensors are based, thus, cannot be used for the conversion of electrical or optical signals to mechanical. Accordingly, they are unsuitable for the generation of structure-borne sound.

In contrast, the phenomena underlying the second group of sensors, the so-called electro-mechanical transducers, are reciprocal and, hence, can be used both as sensors and exciters, disregarding the phase. As an inevitable consequence, this group always is accompanied by some reaction from the electrical side onto the mechanical.

8.2.1 Electrical Sensors

Sensors that control electrical circuits without producing a mechanical reaction act on the electrical circuits by virtue of a relative displacement $\Delta\xi$, which, in principle, is frequency independent even down to the static state.

The most commonly employed principles involve a change in one of the basic electrical two-poles, a resistor, an inductance or a capacitance.

A carbon microphone such as those previously used in telephones, is an example of a sensor that depends on a change in electrical resistance. The displacement of a membrane compresses the carbon aggregates against a rigid housing and this compression increases the aggregate contact area, which thus reduces the resistance. With a few volts from a battery across the aggregate, the $\Delta\xi$ quantities may be converted to directly measurable current changes Δi. Although the sensitivity is so high that no additional amplifier is required, it is rather unstable and generates so much self-noise that it is not useful for structure-borne sound measurements. On the other

hand, sheets of pressure-moulded carbon or graphite are occasionally used for this purpose. Because such sheets are relatively stiff, they are suitable for high frequency tuned acceleration sensors or load transmitting force transducers if their modulus of elasticity is known.

Such a transducer configuration used as a force gauge suffers from the fundamental disadvantage that the electrical resistance

$$R = \rho_{el} \frac{l}{S}, \tag{8.34a}$$

where ρ_{el} denotes the resistivity, and the reciprocal of the stiffness i.e., the compliance

$$\frac{1}{s} = \frac{l}{ES}, \tag{8.34b}$$

depend on the length l and cross-sectional area S in the same way. For force measurements, however, the compliance usually should be small and the resistance large. It is therefore advantageous to separate the resistance element from that determining the extension. Thereby, the resistance element can be made of a thin wire with a large effective length in the direction of the extension, obtained by folding the wire as a serpentine. This design is employed in the modern strain gauge, a typical example of which is shown in Fig. 8.13. For the nine back-and-forth folds shown in the figure, the effective length to be used in (8.34a) is $l = 19l_1$. The lengths l or l_1 appear only, however, in the absolute length changes but not in the strain

$$\frac{\Delta\xi}{l_1} = \frac{\Delta l}{l} = \varepsilon\ . \tag{8.34c}$$

The sensitivity of a strain gauge, defined as the relative change in resistance per unit change of strain, is made up of three contributions, as can be found from Eq. (8.34a)

$$k = \frac{1}{R}\frac{dR}{d\varepsilon} = \frac{1}{l}\frac{\partial l}{\partial\varepsilon} - \frac{1}{S}\frac{\partial S}{\partial\varepsilon} + \frac{1}{\rho_{el}}\frac{\partial\rho_{el}}{\partial\varepsilon}\ . \tag{8.35a}$$

The first term is equal to unity, as follows from the definition of strain. The cross-sectional contraction accounted for by the second term, amounts to 2μ. This means that the sensitivity reduces to

$$k = 1 + 2\mu + \frac{1}{\rho_{el}}\frac{\partial\rho_{el}}{\partial\varepsilon}, \tag{8.35b}$$

giving typical sensitivities between 1.6 and 5.

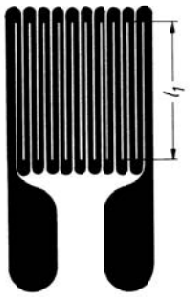

Fig. 8.13. Typical resistance strain gauge

The primary use of strain gauges is the direct sensing of strains of test objects and not in special force transducers. The additional force required to induce a strain in such a gauge itself is generally negligible. Similarly, only for measurements on very thin plates in bending, the slightly elevated location of the gauge from the plate surface of primary interest may require some consideration.

It is common practice to use a strain gauge as one branch of a balanced Wheatstone resistance bridge as depicted in Fig. 8.14 and to find the strain by measuring the bridge current. By appropriate use of several strain gauges in different branches of the Wheatstone bridge, also, various types of deformation can be separated. For example, strain gauges I and II that are glued to the top and bottom of a bar or plate, as shown in Fig. 8.14b, yield the extensional strain if they are connected in branches A and D of the bridge in Fig. 8.14a but indicate the bending strain if they are connected in neighbouring branches such as A and B.

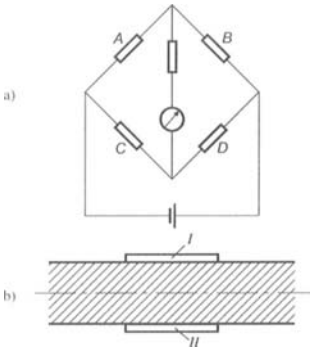

Fig. 8.14. Two resistance strain gauges a) in a bridge circuit and b) attached to a plate

The sensitivity is substantially increased by use semi-conductors. This is on behalf of larger temperature sensitivity than for resistors or common resistance strain gauges.

Sensors making use of inductance changes involve somewhat heavier elements, even if they consist of only two coils that move relative to each other. By using ferrous elements, greater inductance changes, of course, can be obtained but then also the non-linearities and losses resulting from the associated hysteresis phenomena.

Test objects of iron or steel may serve as mobile armatures, the motion of which change the resistance of a magnetic circuit as further discussed in Sect. 8.3.4.

A more reliable and easily implemented system makes use of a rod that is pressed lightly against the test object by a soft pre-compressed spring. Only the end of the rod need be magnetic. When the test object is at rest, this magnetic end should be approximately equally entered in the two coils that constitute the two neighbouring branches of an inductance bridge cf., Fig. 8.15. If the rod is displaced by an amount ξ that is not too large, the inductance of one branch is increased whereas the other is decreased and the current in the bridge is proportional to the displacement ξ or to the practically equally large differential displacement ξ_Δ for a sensor with a low natural frequency.

Since the reactance changes are observed, an alternating voltage must be supplied to the bridge. The frequency of this voltage is called the "carrier

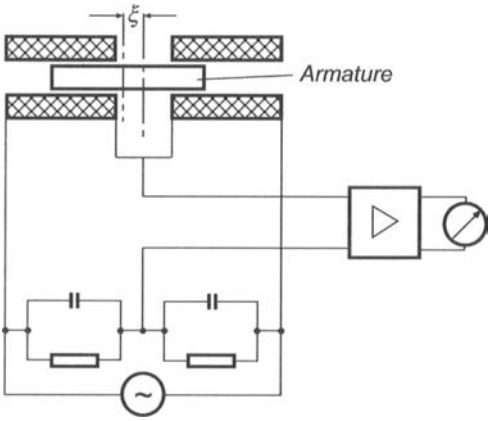

Fig. 8.15. Configuration and circuit of a variable inductance sensor

frequency". The displacement ξ thus is observed in terms of a change in the amplitude of an alternating current at the carrier frequency.

This carrier frequency approach has such great advantages that it is also used for resistance strain gauges. By use of appropriate frequency band filters, the interference or noise at other frequencies can be largely eliminated. In this process, however, the three components making up the "modulated" carrier current must be taken into account, as is seen from the identity

$$\left(A + a\cos\omega t\right)\cos\Omega t = A\cos\Omega t + \frac{a}{2}\left(\cos(\Omega - \omega)t + \cos(\Omega + \omega)t\right). \qquad (8.36)$$

This means that the filters must be chosen such that the entire band $(\Omega - \omega)/2\pi$ to $(\Omega + \omega)/2\pi$ is passed. The carrier frequency, also, always must be kept considerably above the highest frequency to be measured in order to minimize distortion. With a carrier frequency of 4000 Hz, for example, events of frequencies of up to 1000 Hz can be reproduced without distortion.

Instead of using a variable inductance as an element in a circuit, connected to a constant frequency alternating voltage source, the inductance can be used as part of an electric oscillator circuit, the natural frequency of which depends on the inductance L and the capacitance C as

$$\omega_0 = 1/\sqrt{LC}\,. \qquad (8.37)$$

A feedback amplifier may be employed to keep the circuit oscillating at its natural frequency. Because of the non-linearities mentioned above, such arrangements are used less with variable inductances than with variable conductances, as illustrated in Fig. 8.16.

A variable capacitance sensor in its simplest form consists of two metal surfaces of area S, parallel to each other, one of which may be part of the test object or simply a glued-on foil. For small displacements ξ, the changes in the capacitance can be considered approximately linear such that one can write

$$C = C_{eq}\frac{d}{d - \xi} \approx C_{eq}\left(1 + \frac{\xi}{d}\right), \qquad (8.38)$$

where C_{eq} represents the equilibrium value of the capacitance. Variations of ξ thus leads to alterations of the capacitance and thence a frequency modulation, which can be further, processed by means of a signal analyser.

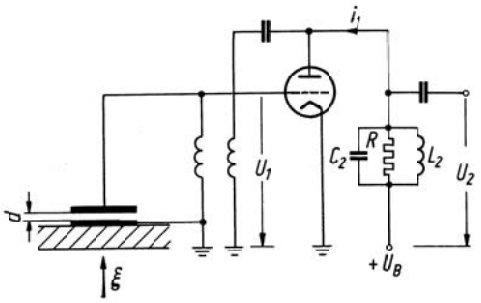

Fig. 8.16. Configuration and circuit of a variable capacitance sensor

This technique, which originally was developed for microphones, allows measurements of excursions as small as 10^{-8}m. The utility of the method, however, is restricted essentially to laboratory investigations, because the equilibrium separation d has a very important effect and must be accounted for by calculations or by electrical compensation. In addition, the capacitance of the sensor is usually so small that unavoidable capacity changes in cables can induce spurious modulations.

In fact, it is important to note that all the phenomena that can be harnessed for sensors, also, can contribute to extraneous signals. From this point of view, a carbon microphone is simply a random aggregate of knife switches.

8.2.2 Optical Sensors

In conjunction with the rather simplified arrangements in Figs. 8.1 and 8.2, it was pointed out that optical means allow measurements of vibration amplitudes using microscope, mirror or stroboscopic light. Also interferometric arrangements can be used, in particularly for calibration purposes. The reflected light beams from an immobile and a vibrating, reflecting surface, are brought to interference so that a fringe pattern results and the amplitude can be determined from the number of fringes and knowledge of the wavelength of the light.

With the laser and the fibre optics, a new avenue for measurements of structure-borne sound is opened. The so-called laser-doppler-vibrometer (LDV) establishes a robust equipment. It uses the fact that a moving reflector realizes a frequency shift due to the Doppler effect. With f_{light} being the frequency of the impinging light, f_{refl} that of the reflected light, v the vibra-

tion velocity of the reflector and c_{light} the phase velocity of the light, one may write

$$f_{refl} = f_{light}\left(1 \pm \frac{v}{c_{light}}\right). \tag{8.39}$$

Since v is of the order of 10^{-3} m/s or smaller and the phase velocity of the light is $3 \cdot 10^8$ m/s, the frequency deviation is extremely small. Modern opto-electronic devices, however, can discriminate such small differences and furnish an electrical signal, which similar to signals from electrodynamic transducers, can be amplified, filtered and stored [8.3].

Figure 8.17 shows the principal design of an LDV. The complete optics is enclosed in a manageable measurement head, which can be used as a non-contacting and interaction-free device in the vicinity of the vibrating object. It should be noted that, again, an immobile reference or a seismic mass is required since a velocity difference is registered between the measurement head and the test object.

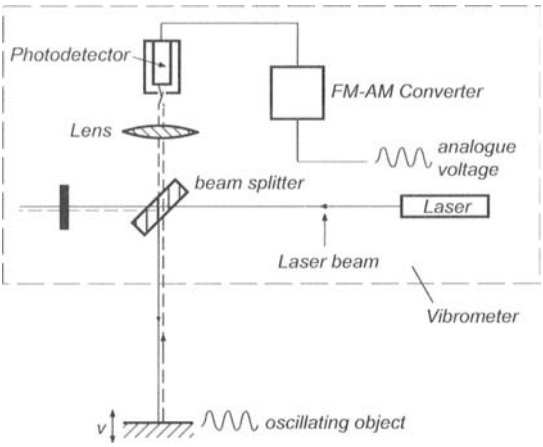

Fig. 8.17. Principle design of a laser-doppler-vibrometer

In Fig. 8.18, yet another principle is outlined for structure-borne sound measurements. In this case a vibrating surface deflects a narrow light beam and establishes a modulation of the light energy impinging on the second optical fibre.

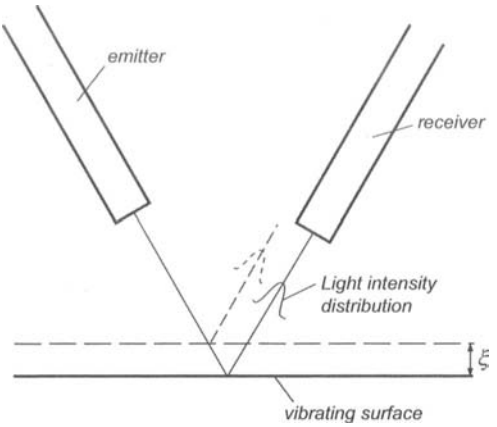

Fig. 8.18. Amplitude modulation of a narrow light beam from a reflecting vibrating surface

In conjunction with optical methods, also, the vibration holograms should be mentioned. Such holograms are either developed as time averaged or double-pulse holograms, which yields more or less easily interpretable pictures of the vibration field. Whereas all other measurement techniques furnish the vibration at a single measurement position, a vibration hologram 'in one go' offers the distribution of an area. Despite this obvious advantage, the snarl in post-processing the holograms has promoted the scanning technique, for instance, employing the laser-doppler-vibrometer, yielding a very good representation of the vibration process.

8.3 Excitation and Measurement of Structure-Borne Sound

For most measurements of structure-borne sound, reciprocal, electromechanical transducers are used in practice. They are based on the electrodynamic, piezo-electric, electro-static or magnetostrictive principles. Their performance is principally determined by the associated transducer constant. Important are additionally their inevitable inner mechanical and electrical impedances as well as the properties of connected elements [8.4-8.6].

8.3.1 Electro-Dynamic Transducers

The fundamental electro-technical principle, upon which, for example, the dynamo is based, states that a loss-free lead of length l_L, which moves with a velocity v_W, perpendicular to its length and to a magnetic field of strength B, establishes a transducer voltage

$$U_w = -Bl_L v_w \,. \tag{8.40a}$$

The velocity v_W is the velocity relative to the magnetic field cf., Fig. 8.19. The transducer constant Bl_L, in this case, has the units Vs/m = Ws/Am and a typical value is 10 Vs/m for structure-borne sound exciters and sensors. The sign is principally arbitrary but in this context it is chosen such that both the electric and the mechanical powers are positive when transmitted to the transducer.

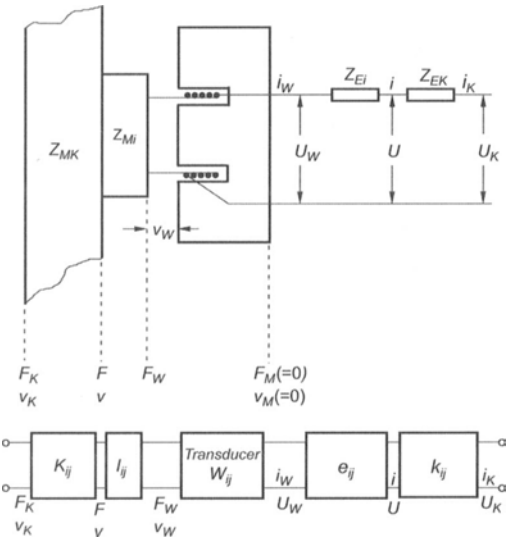

Fig. 8.19. Electrical and mechanical impedances for an electro dynamic transducer. a) Configuration outline and b) generalization as cascaded four-poles

Another fundamental electro-technical principle, underlying, for instance, the electro-motor, states that a current i_w that is passed through a lead of length l_L at rest, perpendicular to magnetic field of strength B, induces a transducer force

$$F_w = Bl_L i_w \,, \tag{8.40b}$$

acting perpendicular to B and i_w.

In phasor notation, Eqs. (8.40) can be rewritten in matrix form as the four-pole equations

$$\begin{Bmatrix} \underline{F}_w \\ \underline{v}_w \end{Bmatrix} = \begin{bmatrix} Bl_L & 0 \\ 0 & -1/Bl_L \end{bmatrix} \begin{Bmatrix} \underline{i}_w \\ \underline{U}_w \end{Bmatrix} . \tag{8.40c}$$

By means of this expression, however, the physical transducer is not described adequately since the loss-free and the motion-less lead clearly is an idealization. The description thus must be augmented by the effects of the mechanical and electrical impedances of the transducer.

For the electrical part, the situation is relatively simple because the transducer is connected in series to the inner electrical impedance consisting of a self-inductance L_i and a resistance R_i such that $Z_{Ei} = j\omega L_i + R_i$. According to Fig. 8.19 the relation

$$\begin{Bmatrix} \underline{i}_w \\ \underline{U}_w \end{Bmatrix} = \begin{bmatrix} 1 & 0 \\ -Z_{Ei} & 1 \end{bmatrix} \begin{Bmatrix} \underline{i} \\ \underline{U} \end{Bmatrix} \tag{8.41a}$$

exists between the transducer quantities i_w and U_w and the physically measurable voltage and current. This relation states that the current through the coil remains unaltered whereas the transducer voltage differs from the measurable by the voltage drop over the inner impedance. Usually, there is externally yet another impedance to consider, for example, that of the measurement equipment connected. Aligned with the arrangements outlined in Fig. 8.19 this means that

$$\begin{Bmatrix} \underline{i} \\ \underline{U} \end{Bmatrix} = \begin{bmatrix} 1 & 0 \\ -Z_{EK} & 1 \end{bmatrix} \begin{Bmatrix} \underline{i}_K \\ \underline{U}_K \end{Bmatrix} . \tag{8.41b}$$

For the mechanical part, the influence of the inner impedance is somewhat more involved. Therefore, the simple case of a rigidly fixed magnet ($v_M = 0$) is considered first and subsequently the more general case.

8.3.1.1 Impedances and Transfer Functions for Immobile Magnets

By excitation of light-weight structures, it is possible to presume that the magnet in Fig. 8.19 is so heavy or fixed to a rigid body such that the magnet velocity v_w equals zero. This is particularly true for loudspeakers, which are nothing but structure-borne sound exciters driving a light membrane and the fluid in front.

With the assumption that the different elements are rigidly connected i.e., the coil and membrane of impedance Z_{Mi} are connected to the measurement object of impedance Z_{MK}, the arrangement in Fig. 8.19 leads to

$$\underline{F}_K - \underline{F} = \underline{Z}_{MK}\,\underline{v}_K\,,\quad \underline{F} - \underline{F}_w = \underline{Z}_{Mi}\,\underline{v}_w\,,\quad \underline{v} = \underline{v}_K = \underline{v}_w. \tag{8.41c}$$

This can also be rewritten in matrix form as

$$\begin{Bmatrix} \underline{F}_K \\ \underline{v}_K \end{Bmatrix} = \begin{bmatrix} 1 & \underline{Z}_{MK} \\ 0 & 1 \end{bmatrix} \begin{Bmatrix} \underline{F} \\ \underline{v} \end{Bmatrix},\quad \begin{Bmatrix} \underline{F} \\ \underline{v} \end{Bmatrix} = \begin{bmatrix} 1 & \underline{Z}_{Mi} \\ 0 & 1 \end{bmatrix} \begin{Bmatrix} \underline{F}_w \\ \underline{v}_w \end{Bmatrix}. \tag{8.41d}$$

Herein, Z_{Mi} is an inherent part of the transducers. It is given by the mass of the coil and membrane m_i and the lossy stiffness of the suspension s_i,

$$Z_{Mi} = j\omega m_i + s_i / j\omega\,. \tag{8.41e}$$

Upon combining Eqs. (8.41a), (8.41b) and (8.41d), one obtains

$$\begin{Bmatrix} \underline{F}_K \\ \underline{v}_K \end{Bmatrix} = \frac{1}{Bl_L} \begin{bmatrix} [(Bl_L)^2 + Z_{MS} Z_{ES}] & -Z_{MS} \\ Z_{ES} & -1 \end{bmatrix} \begin{Bmatrix} \underline{i}_K \\ \underline{U}_K \end{Bmatrix}, \tag{8.41f}$$

where $Z_{MS} = Z_{Mi} + Z_{MK}$ and $Z_{ES} = Z_{Ei} + Z_{EK}$ are the sums of the inner and external mechanical and electrical impedances respectively.

Since the expressions above are written in a form of linked four-poles, which can be combined by means of matrix multiplication, the formulae are readily generalizable to

$$\begin{aligned} \begin{Bmatrix} \underline{F}_K \\ \underline{v}_K \end{Bmatrix} &= \begin{bmatrix} K_{11} & K_{12} \\ K_{21} & K_{22} \end{bmatrix} \begin{Bmatrix} \underline{F} \\ \underline{v} \end{Bmatrix} = \begin{bmatrix} K_{11} & K_{12} \\ K_{21} & K_{22} \end{bmatrix} \begin{bmatrix} I_{11} & I_{12} \\ I_{21} & I_{22} \end{bmatrix} \begin{Bmatrix} \underline{F}_w \\ \underline{v}_w \end{Bmatrix} \\ &= \begin{bmatrix} K_{11} & K_{12} \\ K_{21} & K_{22} \end{bmatrix} \begin{bmatrix} I_{11} & I_{12} \\ I_{21} & I_{22} \end{bmatrix} \begin{bmatrix} W_{11} & W_{12} \\ W_{21} & W_{22} \end{bmatrix} \begin{bmatrix} \varepsilon_{11} & \varepsilon_{12} \\ \varepsilon_{21} & \varepsilon_{22} \end{bmatrix} \begin{bmatrix} \kappa_{11} & \kappa_{12} \\ \kappa_{21} & \kappa_{22} \end{bmatrix} \begin{Bmatrix} \underline{i}_K \\ \underline{U}_K \end{Bmatrix}. \end{aligned} \tag{8.42}$$

Thereby, the input quantities of one transducer element connect to those at the output of the adjacent one. This cascading may involve mass-spring elements, wave guides and electrical circuits.

From (8.41f) and (8.42), all the impedances and transfer functions of interest can be computed. For an immobile magnet of an electro-dynamic structure-borne sound transducer, operated short-circuited, the impedance, for example, is obtained as

$$\left.\frac{\underline{F}_K}{\underline{v}_K}\right|_{\underline{U}_K = 0} = Z_{MS} + \frac{(Bl_L)^2}{Z_{ES}}. \tag{8.43a}$$

The mechanical impedance thus consists of a pure mechanical part $Z_{MS} = Z_{Mi} + Z_{MK}$ and the electrical reaction, the latter of which becomes the

more pronounced, the bigger the transducer constant Bl_L and the smaller the electrical load Z_{ES}. For a typical constant of Bl_L = 10 Vs/m and short circuited operation such that $Z_{ES} \approx Z_{Ei} = 1\Omega$ due to an inner coil resistance, the electrical part of the measured total mechanical impedance would amount to 10 Ns/m. As a comparison, a 16 g mass at 100 Hz also presents an impedance of about 10 Ns/m. One may thus conclude that the electrical reaction predominantly is of significance for light-weight structures and low frequencies. It is possible, however, that the impedance at a resonance becomes that small for big and weakly damped structures that the electric part appears as a noticeable additional damping.

For the electrical impedance of a structure-borne sound exciter with no external forces acting i.e., $\underline{F}_K = 0$, the relation in (8.41f) yields

$$\left.\frac{\underline{i}_K}{\underline{U}_K}\right|_{\underline{F}_K=0} = \frac{Z_{MS}}{(Bl_L)^2 + Z_{MS}Z_{ES}}. \tag{8.43b}$$

This expression is composed of one pure electrical part and a mechanical reaction. Hence, it is, in principle, possible to infer the mechanical impedance from the voltage and current.

The transfer function during operation is also found from (8.41f), again, with no external forces present,

$$\left.\frac{\underline{v}_K}{\underline{U}_K}\right|_{\underline{F}_K=0} = \frac{-Bl_L}{(Bl_L)^2 + Z_{MS}Z_{ES}}. \tag{8.43c}$$

Furthermore, it follows from (8.41c) that $\underline{F} = -Z_{MK}\,\underline{v}_K$ and by substitution in (8.43c), the force exerted by the moving coil on a structure with the impedance Z_{MK} is found to be given by

$$\left.\frac{\underline{F}}{\underline{U}_K}\right|_{\underline{F}_K=0} = \frac{Bl_L Z_{MK}}{(Bl_L)^2 + Z_{MS}Z_{ES}}. \tag{8.43d}$$

For loudspeakers and exciters, acting on very light-weight structures i.e., $Z_{MS} \approx Z_{Mi}$, the resulting velocity is of primary interest. It is given by (8.43c). With a softly suspended moving coil of impedance $Z_{MS} = j\omega m\,(1 - \omega_R^2/\omega^2)$, a frequency characteristic is obtained as outlined in Fig. 8.20, assuming an electric impedance as given by (8.43b). In the graphs, ω_R is the resonance frequency of the mass-spring system made up by the moving coil and the stiffness of the suspension.

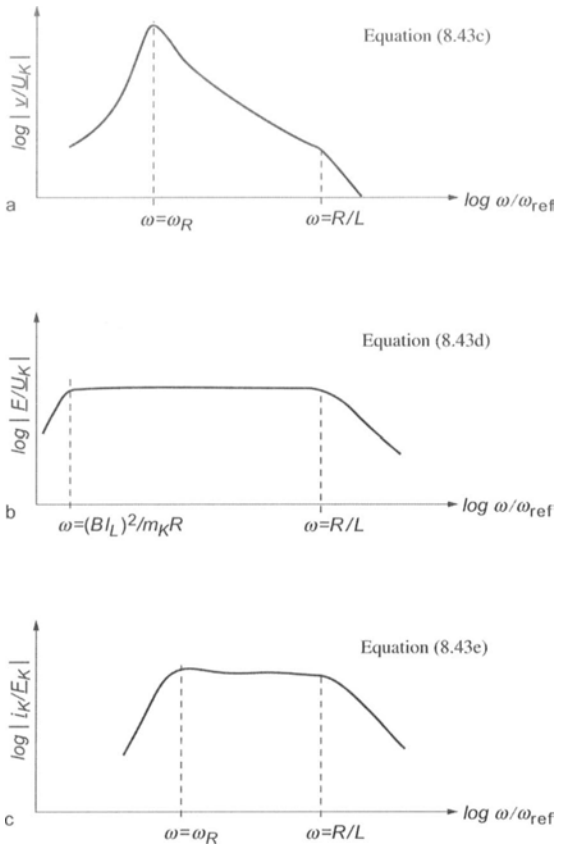

Fig. 8.20. Transfer function of electro-dynamic transducers. a) Exciter ($\underline{F}_K = 0$) with negligible mechanical load, b) exciter ($\underline{F}_K = 0$) with high mechanical load and c) sensor ($\underline{U}_K = 0$) with negligible mechanical load. For high mechanical load, the transfer function is uniform cf., Eq. (8.43f)

For structure-borne sound exciters acting on heavy structures, $Z_{MK} = j\omega m_K >> Z_{Mi}$ and with $Z_{ES} = R + j\omega L$, Eq. (8.43d) renders the middle graph in Fig. 8.20.

Operated as a sensor, the describing transfer function can also be developed from (8.41f). In this situation, however, $\underline{U}_K = 0$ and

$$\left.\frac{\underline{i}_K}{\underline{F}_K}\right|_{\underline{U}_K=0} = \frac{Bl_L}{(Bl_L)^2 + Z_{MS}Z_{ES}}. \tag{8.43e}$$

With the exception of the sign, the right-hand side is identical to that of (8.43c) owing to reciprocity. The design criteria, however, lead to different

transition frequencies. Whereas comparatively large masses can be tolerated for exciters such that ω_R, where $Z_{MK} \to 0$, can be tuned to low frequencies, this is not possible for sensors designed to be very light-weight. In the latter case, the resonance frequency is placed at the centre of the frequency range of interest and the mechanical and electrical damping is made that high that the frequency characteristics in the bottom graph in Fig. 8.20 result. The most important example is the condenser microphone where the exciting force is given by the pressure. Such microphones can be made extremely small owing to the limited load Z_{MS} from the ambient air.

For structure-borne sound sensors, aimed at measuring the velocity of heavy structures, (8.41f) gives

$$\left.\frac{\underline{i}_K}{\underline{v}_K}\right|_{\underline{U}_K=0} = \frac{Bl_L}{Z_{ES}} \quad , \quad \left.\frac{\underline{U}}{\underline{v}_K}\right|_{\underline{U}_K=0} = \frac{Bl_L Z_{EK}}{Z_{ES}}. \tag{8.43f}$$

Up to the decay above $\omega = R/L$, a uniform signature can be established.

8.3.1.2 Energy Balance

In this section it is demonstrated that the equality of the transducer constants in (8.40a) and (8.40b) is a consequence of energy conservation. In this pursuit, quite generally one may write

$$\underline{F}_w = \alpha \underline{i}_w \,, \; \underline{U}_w = \beta \underline{v}_w. \tag{8.44a}$$

In combination with (8.41a) and (8.41c), the physically measurable quantities are obtained as

$$\begin{aligned} \underline{F} &= \underline{F}_w + Z_{Mi}\underline{v} = \alpha \underline{i} + Z_{Mi}\underline{v}, \\ \underline{U} &= \underline{U}_w - Z_{Ei}\underline{i} = \beta \underline{v} - Z_{Ei}\underline{i}. \end{aligned} \tag{8.44b}$$

The mechanical power transmitted is obtained as

$$W_M = \frac{1}{2}\mathrm{Re}\left[\underline{F}\underline{v}^*\right] = \frac{1}{2}\mathrm{Re}\left[\alpha i v^* + Z_{Mi}|\underline{v}|^2\right], \tag{8.44c}$$

and, similarly, the electrical power is

$$W_E = \frac{1}{2}\mathrm{Re}\left[\underline{i}\underline{U}^*\right] = \frac{1}{2}\mathrm{Re}\left[\beta^* \underline{i}\underline{v}^* + Z_{Ei}|\underline{i}|^2\right]. \tag{8.44d}$$

In these expressions, $\mathrm{Re}\left[Z_{Mi}\right]|\underline{v}|^2/2$ and $\mathrm{Re}\left[-Z_{Ei}\right]|\underline{i}|^2/2$ are the dissipated powers by inner mechanical and electrical impedances. The two remaining terms must sum up to zero given the sign convention since ideal transducers neither produce nor dissipate power. Accordingly, one obtains

$$0 = \frac{1}{2}\mathrm{Re}\left[\alpha \underline{i v}^{*}\right] + \frac{1}{2}\mathrm{Re}\left[\beta^{*} \underline{i v}^{*}\right], \qquad -\alpha = \beta^{*}, \tag{8.44e}$$

respectively. If therefore, $\alpha = Bl_L$ it follows that $\beta = - Bl_L$ in accordance with (8.40a).

8.3.1.3 Impedances and Transfer Functions for Mobile Magnets

Upon trying to excite a concrete plate or a heavy machine at low frequencies by means of a handheld, several kg heavy exciter, it is realized that the assumptions made in the previous section of $v_M = 0$ or equivalently $v_w = v$ cf., Fig. 8.18, do not reflect reality. It is obvious that the important effect in exciting low mobility structures at low frequencies, must be taken into account. Whilst all other elements of the transducer remain, only new coefficients I_{ij} in the chain of matrices need be established, linking F_w, v_w and F,v.

For this purpose, Fig. 8.21 presents the essential parts of the transducer together with the forces and velocities. Additionally is introduced a common spring of stiffness s, representing the moving coil suspension s_1 and that suspending the magnet s_2. This means that

$$\begin{aligned} \underline{F} - \underline{F}_w &= Z_{Mi}\,\underline{v} + \frac{s}{j\omega}(\underline{v} - \underline{v}_M), \\ \underline{F}_w - \underline{F}_M &= Z_{MM}\,\underline{v}_M - \frac{s}{j\omega}(\underline{v} - \underline{v}_M), \\ \underline{v}_w &= \underline{v} - \underline{v}_M . \end{aligned} \tag{8.45}$$

Herein, $\underline{F}_w$ again is the transducer force and $\underline{v}_w$ the velocity difference between that of the moving coil and the magnet. Z_{MM} is the impedance of the magnet. In the following it is assumed that $F_M = 0$, which does not imply any restrictions since if the magnet is supported by another structure merely the value of Z_{MM} must be raised and additional resonances considered.

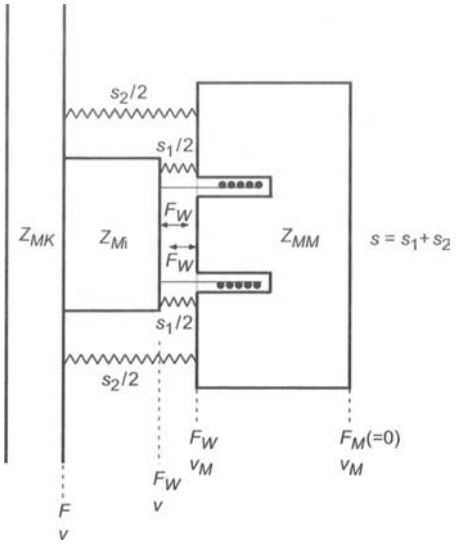

Fig. 8.21. Velocities and forces associated with an electro-dynamic transducer with a mobile magnet

By eliminating $\underline{v}_M$ in (8.45) and rewriting the equations such that F and v only appears on the left–hand side and F_w and v_w on the right, the desirable four-pole is established,

$$\begin{Bmatrix} \underline{F} \\ \underline{v} \end{Bmatrix} = \begin{bmatrix} \dfrac{Z_{Mi}+Z_{MM}}{Z_{MM}} & \dfrac{s}{j\omega}\dfrac{Z_{Mi}+Z_{MM}}{Z_{MM}}+Z_{Mi} \\ \dfrac{1}{Z_{MM}} & 1+\dfrac{s}{j\omega Z_{MM}} \end{bmatrix} \begin{Bmatrix} \underline{F}_w \\ \underline{v}_w \end{Bmatrix}. \tag{8.45a}$$

This expression must be substituted in the chain of matrices (8.42) for I_{ij}. The multiplication by the other already known matrices principally yields

$$\begin{Bmatrix} \underline{F}_K \\ \underline{v}_K \end{Bmatrix} = \begin{bmatrix} A_{11} & A_{12} \\ A_{21} & A_{22} \end{bmatrix} \begin{Bmatrix} \underline{i}_K \\ \underline{U}_K \end{Bmatrix}. \tag{8.45b}$$

Of the rather lengthy expressions for the elements A_{ij}, only

$$A_{11} = \frac{1}{Bl_L}\left[(Bl_L)^2 \frac{Z_{MS}+Z_{MM}}{Z_{MM}} + Z_{ES}Z_{MS}\left(1+\frac{s}{j\omega}\frac{Z_{MS}+Z_{MM}}{Z_{MS}Z_{MM}}\right)\right]$$

and

$$A_{21} = \frac{Z_{ES}}{Bl_L}\left(1 + \frac{s}{j\omega}\frac{1}{Z_{MM}}\right) + \frac{Bl_L}{Z_{MM}}$$

are required for the transfer function. As before, $Z_{MS} = Z_{Mi} + Z_{MK}$ and $Z_{ES} = Z_{Ei} + Z_{EK}$ with the notation given in Fig. 8.19. Upon assuming that Z_{MS} and Z_{MM} can be approximated as mass impedances, one obtains

$$A_{11} = \frac{1}{Bl_L}\left[(Bl_L)^2 \frac{m_{MS} + m_{MM}}{m_{MM}} + Z_{ES}\, j\omega m_{MS}\left(1 - \frac{\omega_{MS}^2}{\omega^2}\right)\right]. \tag{8.45c}$$

The resonance frequency ω_{MS} is that of the mass-spring-mass system constituted by the mass m_{MS} of the structure and the moving coil, the stiffness s of the spring and the mass m_{MM} of the magnet.

The transfer functions when the transducer is operated as exciter, follow from (8.45b) as

$$\begin{aligned} \left.\frac{\underline{v}_K}{\underline{U}_K}\right|_{\underline{F}_K = 0} &= \frac{-A_{12}A_{21}}{A_{11}} + A_{22} = \frac{A_{11}A_{22} - A_{12}A_{21}}{A_{11}} = -\frac{1}{A_{11}} \\ \left.\frac{\underline{F}}{\underline{U}_K}\right|_{\underline{F}_K = 0} &= \frac{Z_{MK}}{A_{11}} \end{aligned}, \tag{8.45e}$$

and operated as sensor

$$\begin{aligned} &\left.\frac{\underline{i}_K}{\underline{F}_K}\right|_{\underline{U}_K = 0} = \frac{1}{A_{11}} \\ &\left.\frac{\underline{i}_K}{\underline{v}_K}\right|_{\underline{U}_K = 0} = \frac{1}{A_{21}}, \quad \left.\frac{\underline{U}}{\underline{v}_K}\right|_{\underline{U}_K = 0} = \frac{Z_{EK}}{A_{21}}. \end{aligned} \tag{8.45f}$$

In the first of these expressions, use is made of the fact that the determinant of the transducer matrix in (8.40c) equals –1. The other matrices in (8.42) have all unity determinants. This means that the determinant of the chain of matrices becomes

$$A_{11}A_{22} - A_{12}A_{21} = (+1)\cdot(+1)\cdot(-1)\cdot(+1)\cdot(+1) = -1.$$

From the transfer functions in (8.45e,f), the following conclusions can be drawn:

- When the spring is very stiff, ω_{MS} falls relatively high. In the range $\omega < \omega_{MS}$ almost nothing moves and almost no force is exerted on the test object.

- When ω_{MS} is tuned sufficiently low in frequency, which is the usual design, the transfer functions turns into the corresponding expressions in (8.43d) to (8.43f) for $Z_{MM} > Z_{MS}$.
- For structure-borne sound exciters, the motion of the magnet leads to an elevation of the lower frequency limit at $|Z_{MS}| = (Bl_L)^2 / |Z_{ES}|$ in Fig. 8.20b by a factor of $|1 + Z_{MS}/Z_{MM}|$. This means that the force diminishes towards low frequencies, which is due to the counter voltage increase induced by the magnet motion. Differently described, the effective electrical resistance increases with the enlarged motion of the magnet through the reaction in (8.43a). In the upper range, the transducer has the frequency characteristics depicted in the figure.

For structure-borne sound sensors according to Fig. 8.11b, the same applies as for exciters. By means of soft springs is pursued, a mass-spring-mass resonance as low as possible. A resonance frequency of 5 Hz or below is fully realistic.

From the expressions and the associated discussion it follows that electro-dynamic transducers should be designed with an as large transducer constant and an as low mass-spring-mass resonance as possible. These guide lines become slightly contradictive in practice. A low mass-spring-mass resonance requires a very soft spring and a large Bl_L product requires a very narrow air gap in the magnet, which can be achieved only by means of a stiff coil suspension in order to prevent the coil from touching the magnet. This problem is usually solved through a multi-stage suspension, which is soft in the direction of motion but avoids sidewise and rocking motion of the moving coil.

For modern electro-dynamic exciters, one may typically assume a maximum long-term force of 5 to 10 N per kg exciter mass. A larger force could be achieved, in principle, through a higher current but this would result in too high a heat release without external cooling.

In many applications it is interesting to know the relation between the transducer force $\underline{F}_w$ and magnet velocity $\underline{v}_M$. It is presumed thereby that the transducer is operated as a sensor such that Eqs. (8.45) takes the form

$$\begin{aligned} Z_{MK}\,\underline{v} - \underline{F}_w &= Z_{Mi}\,\underline{v} + \frac{s}{j\omega}(\underline{v} - \underline{v}_M) \\ \underline{F}_w - 0 &= Z_{MM}\,\underline{v}_M - \frac{s}{j\omega}(\underline{v} - \underline{v}_M). \end{aligned} \tag{8.46}$$

By eliminating $\underline{v}$, the relation is obtained

$$\underline{v}_M = \underline{F}_w \frac{Z_{MS}}{Z_{MS}Z_{MM} + \dfrac{s}{j\omega}(Z_{MS} + Z_{MM})} = \frac{\underline{F}_w}{Z_{MM}} \frac{1}{1 + \dfrac{s}{j\omega}\dfrac{Z_{MS} + Z_{MM}}{Z_{MS}Z_{MM}}}. \qquad (8.46a)$$

The second denominator can also be brought in the form $1 - \omega_{MS}^2/\omega^2$. Equation (8.46a) thus states that above the mass-spring-mass resonance, the transducer force $\underline{F}_w$ can simply be determined from the easily measured magnet velocity, multiplied by Z_{MM} cf., Sect. 4.2.

In the present analysis is left aside the mechanical reaction onto the test object by the transducer. This problem was considered in Sect. 8.2.4, particularly in Eq. (8.33). Merely the remark should be made that the transducer impedance required in this context can be obtained from the chain of matrices as $Z_{acc} = \underline{F}/\underline{v}$, which consists of one mechanical and one electrical part as exemplified in Eq. (8.43a). As in many other situations, the analysis demonstrates that splitting a complicated problem in "independent parts", as here in mechanical and electrical parts, certainly conforms to human perception and often performs successfully. At the end of the day, however, the "parts" are coupled and the behaviour and performance always must be assessed for the integrated system.

8.3.2 Piezo-Electric Transducers

Thanks to their manageability, almost exclusively piezo-electric sensors are used for structure-borne sound measurements. The designs of the most important types are outlined in Fig. 8.22. One is here concerned with a transducer responding to acceleration, which up to its resonance frequency has an almost flat response and can be manufactured robust and very small, down to a tenth of a gram. As rough guides can be used a sensitivity of 100 to 1000 m_{acc} [Vs^2/m] and a resonance frequency of $100/m_{acc}$ to $600/m_{acc}$ [Hz] where m_{acc} is the total mass of the transducer.

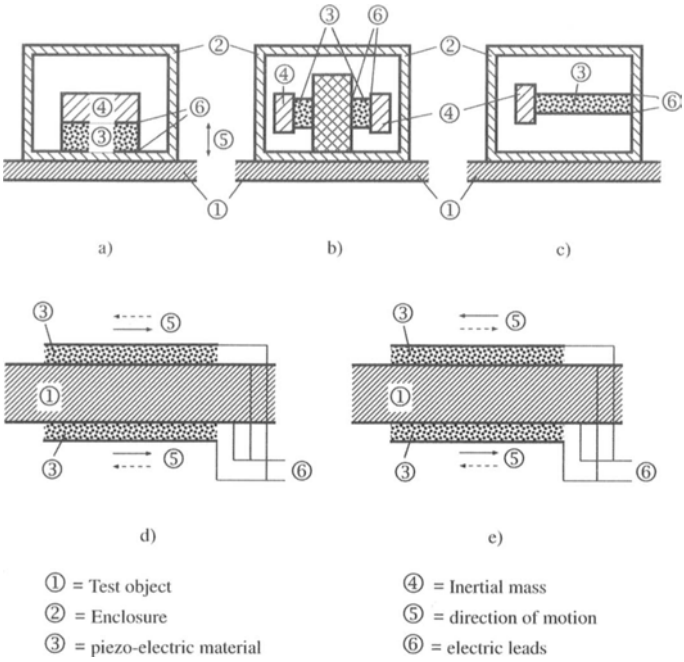

Fig. 8.22. Examples of piezo-electric transducers. a) compressional, b) shear and c) flexural design. d) longitudinal and e) flexural PVDF transducers

The piezo-electric transducer is suitable as exciter only when small displacements but large forces are required. Hence, the transducer must face large impedances on both sides and large voltages must be employed.

More recently, thin piezo-film (PVDF) has become commercially available, which can be glued to the test object and used both as sensor and exciter. As illustrated in Fig. 8.22, longitudinal and flexural waves can be excited with a good bonding. The advantage is that no large masses or stiff suspensions are required as support for the exciter [8.7]. Such piezo-film is manufactured in different thicknesses and thereby, almost non-loading transducers can be achieved. The reproducibility, however, can still be significantly improved.

To understand the piezo-electric effect, one can imagine different positive and negative ions, which are displaced in the material such that a net charge is realized as sketched in Fig. 8.23. In an undeformed state, the ions are in electrical equilibrium so that no charge appears at the externally attached electrodes. This equilibrium is disturbed if the lattice is compressed or stretched corresponding to compressive or tensile strains as in Fig.

8.23b and c respectively. Electric charges then collect at the electrodes, without the requirement of an external source of charges. Due to the Poisson contraction, also a displacement η along the crystal (*y* direction), perpendicular to the crystal axis (*x* direction) can produce such a change in charge. One may therefore assume [8.8] that

$$Q_w = -K_{xx}\xi\,, \quad Q_w = -K_{xy}\eta\,, \tag{8.47}$$

where Q_w is the transducer charge established. ξ and η are the compression and cross-sectional contraction respectively with the associated transducer constants K_{xx} and K_{xy}, dependent on the material, patch size, patch form and alignment with the crystal axis.

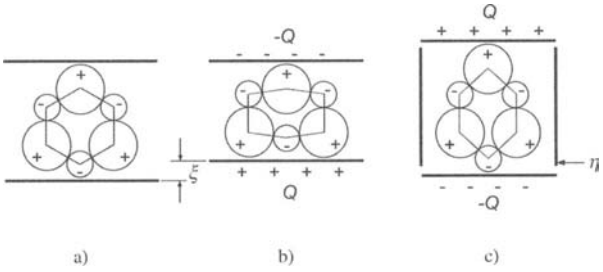

Fig. 8.23. Behaviour of piezo-electric materials [8.4]. a) undeformed state, b) deformation in the direction of (axial) and c) perpendicular to the current (lateral)

In the following only one direction of motion will be considered and therefore a single transducer constant *K* is sufficient. For the analysis must be considered, moreover, that the temporal change in charge is proportional to the current $i = dQ/dt$ and the temporal change in displacement is proportional to the velocity $v = d\xi/dt$. Upon introducing the phasor notation, the first fundamental relation

$$\underline{i}_w = -K\underline{v}_w \tag{8.47a}$$

is obtained for piezo-electric transducers. The reciprocal piezo-electric effect implies that an applied voltage gives rise to a proportional expansion of the material, leading to a mechanical transducer force

$$\underline{F}_w = K\underline{U}_w\,. \tag{8.47b}$$

The fact that the same constant *K* appears in both (8.47a) and (8.47b) is again a consequence of energy conservation. The proof proceeds exactly as for electro-dynamic transducers in (8.44c) to (8.44e).

By combining the last two equations, the four-pole description is obtained as

$$\begin{Bmatrix} \underline{F}_w \\ \underline{v}_w \end{Bmatrix} = \begin{bmatrix} 0 & K \\ -1/K & 0 \end{bmatrix} \begin{Bmatrix} \underline{i}_w \\ \underline{U}_w \end{Bmatrix} \tag{8.48}$$

Since the velocity is proportional to current and force to voltage for piezo-electric transducers whereas the situation is the opposite for electro-dynamic ones, the distinction is made between *N*-transducers in the former case and *M*-transducers in the latter.

Another difference between the two types of transducers is the role of the inner impedance. In Fig. 8.19, this impedance is in series with the transducer, rendering an inevitable voltage drop. For the piezo-electric transducers, in contrast, the capacitance of the transducer is parallel to the current source i_w and, thus, yields a drop in current. Therefore, the transducer circuit is that shown in Fig. 8.24. The associated electrical relations can be compiled as

$$\begin{Bmatrix} \underline{i}_w \\ \underline{U}_w \end{Bmatrix} = \begin{bmatrix} 1 & -1/Z_{Ei} \\ 0 & 1 \end{bmatrix} \begin{Bmatrix} \underline{i} \\ \underline{U} \end{Bmatrix}. \tag{8.49}$$

Herein, Z_{Ei} essentially represents the relatively large impedance of the capacitance realized by the transducer

$$Z_{Ei} = 1/j\omega C\,. \tag{8.49a}$$

Thereby, the matrices in the four-pole chain in Fig. 8.24 are known since the mechanical and electrical loads, again can be taken from (8.41d) and (8.43a) and (8.41b) respectively. By carrying out the matrix multiplication, the mechanical part is found to be described by

$$\begin{Bmatrix} \underline{F}_K \\ \underline{v}_K \end{Bmatrix} = \begin{bmatrix} \dfrac{Z_{MS}+Z_{MM}}{Z_{MM}} & \dfrac{s}{j\omega}\dfrac{Z_{MS}+Z_{MM}}{Z_{MM}} + Z_{MS} \\ 1/Z_{MM} & 1+\dfrac{s}{j\omega Z_{MM}} \end{bmatrix} \begin{Bmatrix} \underline{F}_w \\ \underline{v}_w \end{Bmatrix}, \tag{8.49b}$$

and the electrical part by

$$\begin{Bmatrix} \underline{F}_w \\ \underline{v}_w \end{Bmatrix} = \begin{bmatrix} -KZ_{EK} & K \\ -\dfrac{1}{K}\left(1+\dfrac{Z_{EK}}{Z_{Ei}}\right) & \dfrac{1}{KZ_{Ei}} \end{bmatrix} \begin{Bmatrix} \underline{i}_K \\ \underline{U}_K \end{Bmatrix}. \tag{8.49c}$$

In the mechanical part, $Z_{MS} = Z_{Mi} + Z_{MK}$ is the sum of the mechanical sensor impedance, essentially given by the mass of the housing, and the im-

pedance of the test object. In contrast to the electro-dynamic transducer, Z_{MM} here represents the impedance of the seismic mass.

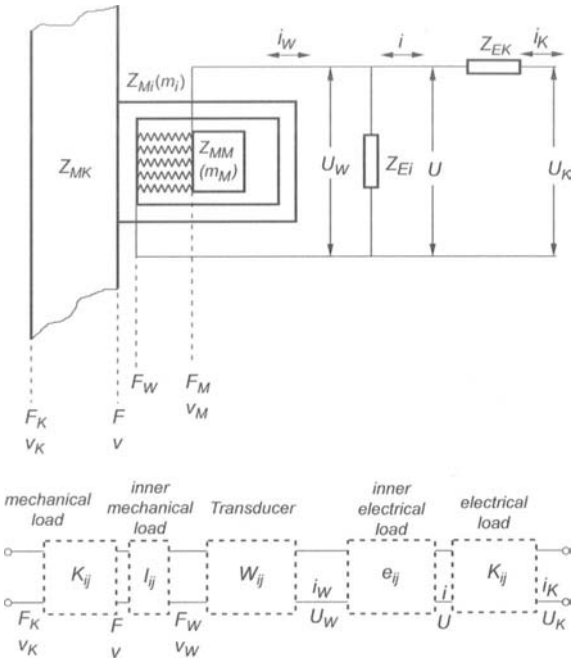

Fig. 8.24. Electrical and mechanical impedances for a piezo-electric transducer. a) Configuration outline and b) generalization as cascaded four-poles

Upon comparing Figs. 8.19 and 8.24, the following correspondences can be made, cf., Sect. 8.3.6.1:

Electro-dynamic transducer	Piezo-electric transducer
Voltage source	Current source
Series connected inner impedance	Parallel connected inner impedance
Magnet impedance Z_{MM}	Seismic mass impedance Z_{MM}

$$Z_{MM} \approx j\omega m_{MM} \tag{8.49d}$$

Soft suspension s	Stiff piezo crystal s
Moving coil impedance Z_{Mi}	Transducer housing impedance Z_{Mi}

$$Z_{Mi} \approx j\omega m_{Mi} \tag{8.49e}$$

A multiplication of (8.49b) and (8.49c) yields the complete matrix, again, in the form of (8.45b). Also in this case, the individual determinants equal ±1. In analogy with (8.45f), the sensor sensitivity is obtained as

$$\left.\frac{\underline{U}}{\underline{v}_K}\right|_{\underline{U}_K=0} = \frac{Z_{EK}}{A_{21}} = \frac{-K}{\left(\frac{1}{Z_{EK}}+\frac{1}{Z_{Ei}}\right)\left(1+\frac{s}{j\omega Z_{MM}}\right)+\frac{K^2}{Z_{MM}}}. \tag{8.50a}$$

For the subsequent discussion it is suitable to let $Z_{MM} = j\omega m_{MM}$, $Z_{Ei} = 1/j\omega C$, $Z_{EK} = R$, which correspond to the usual experience with piezo-electric transducers and to convert from velocity to acceleration. Accordingly, (8.50a) becomes

$$\left.\frac{\underline{U}}{\underline{a}_K}\right|_{\underline{U}_K=0} = \frac{m_{MM}K}{sC}\frac{-1}{\left(1+\frac{1}{j\omega CR}\right)\left(1-\frac{\omega^2 m_{MM}}{s}\right)+\frac{K^2}{sC}}. \tag{8.50b}$$

The second term in the denominator is very small and plays only a role at the resonance frequency $\omega^2 = s/m_{MM}$. In Fig. 8.25a are shown the frequency characteristics of Eq. (8.50b). Since R can be made extremely high with modern charge amplifiers and also the ratio s/m will be high for small accelerometers, the frequency response is essentially constant in a wide frequency range.

Piezo-electric materials are also frequently employed for measurements of dynamic forces. A design of the transducer is shown schematically in Fig. 8.26. The transfer function can be developed from (8.49a) and (8.49b) to be given by

$$\left.\frac{\underline{U}}{\underline{F}_K}\right|_{\underline{U}_K=0} = \frac{-1}{K}\frac{1}{\frac{Z_{MM}+Z_{MS}}{Z_{MM}}+\frac{1}{K^2}\left(\frac{1}{Z_{EK}}+\frac{1}{Z_{Ei}}\right)\left(Z_{MS}+\frac{s}{j\omega}\frac{Z_{MM}+Z_{MS}}{Z_{MM}}\right)} \approx \frac{-1}{K}. \tag{8.50c}$$

The rather simple approximation in the last part of (8.50c) is admissible for the following conditions:

- For force transducers, one is concerned with making the mechanical element between the force to be registered and the piezo-electric element as small but stiff as possible. Therefore, $Z_{MS} = Z_{MK} + Z_{Mi} << Z_{MM}$, where Z_{MM} is the impedance of the excited structure.
- The transducer constant K as well as the electrical impedances Z_{Ei} and Z_{EK} are numerically very large.

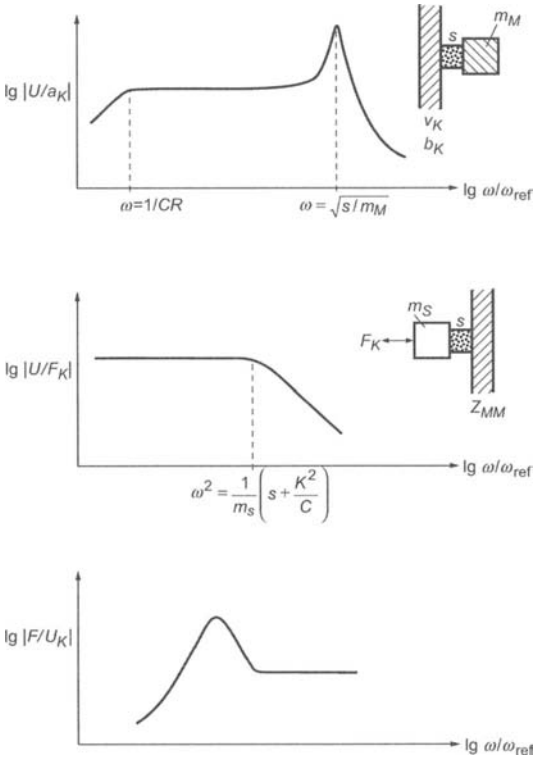

Fig. 8.25. Frequency response of piezo-electric transducers. a) accelerometer as in Fig. 8.23, b) force transducer as in Fig. 8.26 and c) piezo-electric exciter

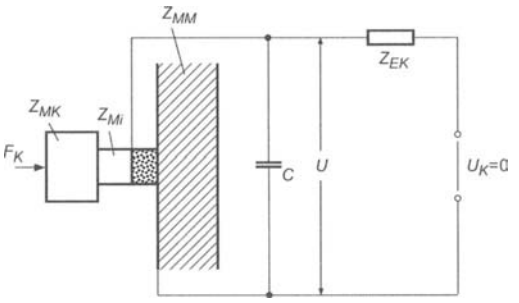

Fig. 8.26. Principle design of piezo-electric force transducer

As pointed out, the piezo-electric materials can also be used for structure-borne sound exciters. In such a case the transfer function is determined from (8.49b) and (8.49c) as

$$\left.\frac{\underline{F}}{\underline{U}_K}\right|_{F_K=0} = \frac{Z_{MK}}{Z_{MS}} \frac{-K}{\left(1+\frac{Z_{EK}}{Z_{Ei}}\right)\left(1+\frac{s}{j\omega Z_T}\right)+\frac{K^2 Z_{EK}}{Z_T}}, \qquad (8.50d)$$

where $Z_T = (Z_{MK} + Z_{Mi} + Z_{MM})/Z_{MM}(Z_{Mi} + Z_{MK})$ and $Z_{MS} = Z_{Mi} + Z_{MK} \approx Z_{MK}$. By substitution of typical data, one can readily convince oneself that piezo-electric exciters do not offer large forces at low frequencies cf., Fig. 8.25c. For frequencies above the mass-spring-mass resonance, where the piezo-electric material acts as a spring, Eq. (8.50d) reduces to -*K* in a wide frequency range.

The choice of suitable piezo-electric materials as well as electrical and mechanical impedances is a crucial aspect of the transducer design. Additionally, a series of other considerations must be made. In this context should be mentioned, the sensitivity to disturbing electrical and magnetic fields, temperature stability (pyro-electric effects), minimal deformation of the transducer housing etc. as well as directional sensitivity.

8.3.3 Electro-Static Transducers

Electrostatic or dielectric transducers most often consist of two plate-like electrodes across which a dc-voltage is supplied. One of the electrodes is very thin and is fixed (glued) to the test object. In accordance with applications in practice, only the situation with an immobile backing electrode as depicted in Fig. 8.27 will be considered. A situation with a mobile backing electrode can be treated as in Sect. 8.3.1.3.

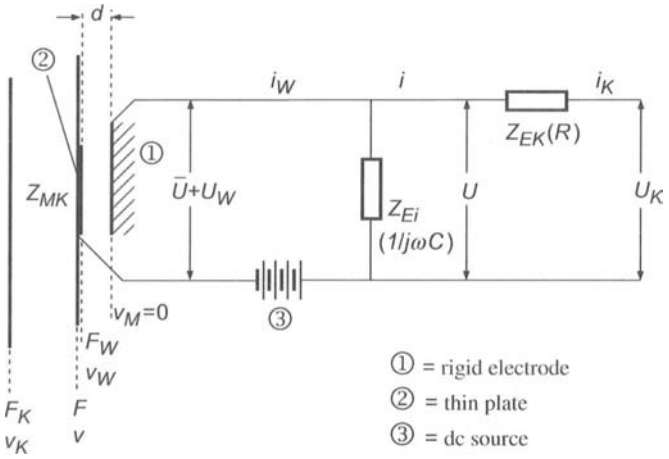

Fig. 8.27. Principle configuration of an electro-static transducer

The condenser microphone for airborne sound is also an electrostatic transducer. It consists of a thin, firmly prestressed membrane constituting one of the electrodes and the rigid housing forming the other. The membrane is forced to vibrations by incident sound whereby its amplitude is converted to an electrical signal by the transducer [8.9].

The electro-mechanical relation underlying this transducer is Coulomb's law of electro-static attraction. Applied on two plates at a distance d with the equilibrium capacitance $\overline{C}$, the attraction force is given by

$$F = \frac{QU}{2d} = \frac{\overline{C}U^2}{2d} = \frac{\overline{C}}{2d}(\overline{U} + \tilde{U})^2 \approx \frac{\overline{C}}{2d}\overline{U}^2 + \frac{\overline{C}}{d}\overline{U}\tilde{U}. \tag{8.51a}$$

Herein, Q is the charge of the condenser, $\overline{U}$ the dc voltage supplied and $\tilde{U}$ the ac voltage.

In the acoustics context, the approximation in (8.51a) corresponding to a linearization is legitimate since the dc voltage supplied usually is of the order of 100 V or more whilst the induced ac voltage is less than a hundredth thereof. The linearization is also valid for the so-called electret transducers, often employed in microphones, for which no external dc voltage is supplied but the transducer material furnishes an internal polarization voltage.

For the exciter problem, only the alternating voltage is of interest and in phasor notation, the transducer force can be written as

$$\underline{F}_w = \frac{\overline{C}\,\overline{U}}{d}\underline{U}_w. \tag{8.51b}$$

This force is exerted on the test object for a constant capacitance $\overline{C}$. In the opposite situation with the transducer as sensor, where the membrane is brought to vibrate with the velocity $\underline{v}_w$, the transducer current amounts to

$$\underline{i}_w = -\frac{\overline{C}\,\overline{U}}{d}\underline{v}_w. \tag{8.51c}$$

In this development, again, the equality of magnitudes of transducer constants, proven in (8.44a) to (8.44e), is used. In the four-pole representation, the equation for ideal electro-static transducers reads

$$\begin{Bmatrix} \underline{F}_w \\ \underline{v}_w \end{Bmatrix} = \begin{bmatrix} 0 & \overline{C}\,\overline{U}/d \\ -d/\overline{C}\,\overline{U} & 0 \end{bmatrix} \begin{Bmatrix} \underline{i}_w \\ \underline{U}_w \end{Bmatrix}. \tag{8.51d}$$

Disregarding the symbols, (8.51d) is identical to the representation for piezo-electric transducers. The close relationship between the two types of transducers is also valid for the influence of the inner electrical impedance.

Also for electro-static transducers, one part of the resulting current passes the inner impedance Z_{Ei} connected in parallel as shown in Fig. 8.27. The inner impedance is essentially capacitive such that Eqs. (8.49) and (8.49d) can be adopted directly.

Regarding the inner mechanical impedance there is a small difference, however. In contrast to electro-dynamic and piezo-electric transducers, a polarization voltage is supplied resulting in an attraction force according to (8.51a). During operation, this force varies, a fact that also can be expressed in terms of an additional, electrically induced stiffness

$$\begin{aligned} s_E &= \frac{dF}{d\xi} = \frac{1}{2d}\frac{dQU}{d\xi} = \frac{\overline{Q}}{2d}\frac{dU}{d\xi} + \frac{\overline{U}}{2d}\frac{dQ}{d\xi} = \frac{\overline{Q}}{2d}\frac{d}{\overline{C}\,\overline{U}}\frac{dF}{d\xi} + \frac{\overline{U}^2}{2d}\frac{dC}{d\xi} \\ &= \frac{1}{2}\frac{dF}{d\xi} + \frac{\overline{U}^2\overline{C}}{2d}\frac{d(1-\xi/d)}{d\xi} = \frac{1}{2}\frac{dF}{d\xi} - \frac{\overline{U}^2\overline{C}}{2d^2} \Leftrightarrow s_E = -\frac{\overline{U}^2\overline{C}}{d^2} = -\left(\frac{\overline{U}\,\overline{C}}{d}\right)^2\frac{1}{\overline{C}} \end{aligned} \tag{8.51e}$$

as developed from (8.51a). Herein, ξ is the change in electrode distance and the variable capacitance is approximated by

$$C = \frac{\overline{C}}{1+\xi/d} \approx \overline{C}(1-\xi/d)\,. \tag{8.51f}$$

As can be expected, s_E is negative since compression implies an enlarged attraction, in contrast to an ordinary mechanical spring. Accordingly, the additional mechanical impedance, resulting in this way, becomes

$$Z_{ME} = \frac{s_E}{j\omega} = -\frac{1}{j\omega\overline{C}}\left(\frac{\overline{U}\,\overline{C}}{d}\right)^2. \tag{8.51g}$$

In this expression, the transducer constant squared appears. This is typical for the mechanical effect of an electrical element as observed in (8.43a).

For the remaining analysis, all the relations, previously derived for the piezo-electric transducers, can be adopted. Only the inner mechanical impedance must be replaced by

$$Z'_{Mi} = Z_{Mi} - \frac{1}{j\omega\overline{C}}\left(\frac{\overline{U}\,\overline{C}}{d}\right)^2. \tag{8.51h}$$

In this way, the chain of matrices becomes

$$\begin{aligned} \begin{Bmatrix} \underline{F} \\ \underline{v} \end{Bmatrix} &= \begin{bmatrix} 1 & Z'_{Mi} \\ 0 & 1 \end{bmatrix}\begin{bmatrix} 0 & \alpha \\ -1/\alpha & 0 \end{bmatrix}\begin{bmatrix} 1 & -1/Z_{Ei} \\ 0 & 1 \end{bmatrix}\begin{Bmatrix} \underline{i} \\ \underline{U} \end{Bmatrix} \\ &= \begin{bmatrix} Z'_{Mi}/\alpha & \alpha + Z'_{Mi}/\alpha Z_{Ei} \\ -1/\alpha & 1/\alpha Z_{Ei} \end{bmatrix}\begin{Bmatrix} \underline{i} \\ \underline{U} \end{Bmatrix}, \end{aligned} \tag{8.52a}$$

in case of an immobile backing electrode. With $Z_{MM} \to \infty$, the transfer function of the transducer operated as a sensor is obtained by means of (8.50a) as

$$\left.\frac{\underline{U}}{\underline{v}_K}\right|_{\underline{U}_K=0} = \frac{\overline{C}\overline{U}Z_{Ei}}{d\left(1+Z_{Ei}/Z_{EK}\right)} \to \frac{-\overline{U}}{j\omega d\left(1+1/j\omega\overline{C}R\right)}. \tag{8.52b}$$

In this development are used the impedances $Z_{Ei} = 1/j\omega\overline{C}$ and $Z_{EK} = R$, in accordance with applications in practice. Upon multiplying both sides by $j\omega$, the left-hand side becomes the ratio of voltage to displacement $\underline{\xi} = \underline{v}/j\omega$. This means that for high impedance signal analysis equipment such that $\omega > 1/RC$, the electro-static transducer constitutes a displacement sensor.

The transducer relations derived in these sections can also be established by means of Hamilton's principle, once again proving its generality. The procedure will be exemplified in this section of electro-static transducers whereby are required the energy of a charged condenser

$$E_C = \frac{1}{2}\frac{Q^2}{C}, \tag{8.53a}$$

and that of an inductance

$$E_L = \frac{1}{2}Li^2 = \frac{1}{2}L\dot{Q}^2, \tag{8.53b}$$

both of which can be obtained from textbooks.

For the model sketched in Fig. 8.28, where the displacement ξ_K is assumed prescribed, the kinetic energies to be considered are $m_K\dot{\xi}^2/2$ and $L\dot{Q}^2/2$ whilst the potential energies read $s\xi^2/2$, $s_K(\xi-\xi_K)^2/2$ and $(\overline{Q}+\tilde{Q})^2/2(\overline{C}+\tilde{C})$. This means that the Hamiltonian becomes

$$\frac{1}{2}\left[m_K\dot{\xi}^2 + L\dot{\tilde{Q}}^2 - s\xi^2 - s_K\left(\xi-\xi_K\right)^2 - \frac{\left(\overline{Q}-\tilde{Q}\right)^2}{\overline{C}}\left(1-\xi/d\right)\right], \tag{8.53c}$$

where both the charge and the capacitance are split in dc and ac components and the vanishing time derivative of $\overline{Q}$ is omitted. In the last term, moreover, the displacement dependent ac component of the capacitance is approximated according to (8.51d).

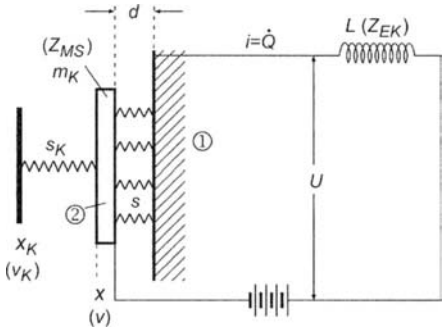

Fig. 8.28. Model of electro-static transducer showing the notation used in Eqs. (8.51) to (8.54). The backing electrode (1) and the mass (2) form a capacitor

Upon carrying out the variation with respect to the unknown co-ordinates ξ and $\tilde{Q}$, one obtains

$$\begin{aligned} &m_K\ddot{\xi} + s\xi + s_K\left(\xi - \xi_K\right) - \frac{\left(\overline{Q}+\tilde{Q}\right)^2}{2\overline{C}d} = 0, \\ &L\ddot{\tilde{Q}} + \frac{1}{\overline{C}}\left(\overline{Q}+\tilde{Q}\right)\left(1-\xi/d\right) = 0. \end{aligned} \tag{8.54a}$$

The subsequent manipulations are:

- Omission of terms of second order e.g., $\xi\dot{\tilde{Q}}$.
- Change to velocity $v = \dot{\xi}$ and current $i = \dot{\tilde{Q}}$ implying that all dc components vanish.
- Introduction of phasor notation i.e., $\ddot{\xi} = j\omega\underline{v}$, $\ddot{\tilde{Q}} = j\omega\underline{i}$.
- Substitution of the inductive impedance $j\omega L$ by Z_{EK} and the mass and spring impedance by Z_{Mi} such that, simultaneously, the result becomes more general and losses can be taken into account.

The outcome of these operations is

$$\begin{aligned} &Z_{Mi}\underline{v} + \frac{s_K}{j\omega}\underline{v} - \beta\,\underline{i} = \frac{s_K}{j\omega}\underline{v}_K, \\ &\beta\,\underline{v} - \left(Z_{EK} + \frac{1}{j\omega\overline{C}}\right)\underline{i} = 0, \end{aligned} \tag{8.54b}$$

where the abbreviation $\beta = \overline{Q}/j\omega d\overline{C} = \overline{U}/j\omega d$ has been introduced. Clearly the first expression has the dimension of force whereas the second that of voltage. Therefore, this set of equations can be compared with that in (8.52a). By observing that the force and the voltage are $\underline{F} = s_K(\underline{v}_K - \underline{v})/j\omega$ and $\underline{U} = Z_{EK}\underline{i}$ respectively, Eq. (8.54b) can be rewritten as

$$\begin{aligned} \underline{F} &= Z_{Mi}\,\underline{v} - \beta\,\underline{i}, \\ \underline{U} &= \beta\,\underline{v} + \underline{i}\,/\,j\omega\overline{C}. \end{aligned} \tag{8.54c}$$

It is somewhat laborious to bring (8.54c) in the form of (8.52a) since the difference between Z_{Mi} and Z'_{Mi} need be considered. If, in spite of that, the algebra is undertaken, it is found that both methods yield the same result with the exception of the sign of the current i, associated with the sign convention.

A comparison of the two procedures shows that the one based on Hamilton's principle is the least transparent and that, in the present formulation, the electrical and mechanical losses can be taken into account only afterwards. On the other hand, however, it has the advantage of starting from very fundamental relations as well as automatically accounting for the equality in transducer constants, the influence of the inner impedances and the significance of the additional, electrically induced stiffness.

8.3.4 Electro-Magnetic Transducers

For electro-magnetic transducers, the ferromagnetic armature is located in a magnetic field with a large flux as depicted in Fig. 8.29. The force acting between the magnet and the armature, is proportional to the flux squared,

$$F \propto \Phi^2 \propto \left(\overline{\Phi} + \tilde{\Phi}\right)^2. \tag{8.55a}$$

To establish a linear relationship between the electrical and mechanical variables, again, a large dc component $\overline{\Phi}$ is required. It can be achieved by means of a permanent magnet or a coil supplied with a direct current. Superimposed on the direct component is an alternating. Operated as an exciter, the latter is the alternating current through the coil and as a sensor, it is ultimately the perturbations of the reluctance due to the changes in the distance d, which give rise to an alternating flux $\tilde{\Phi}$. Because the transducer is reversible, the ideal transducer relations are given by

$$\begin{Bmatrix} \underline{F}_w \\ \underline{v}_w \end{Bmatrix} = \begin{bmatrix} \gamma & 0 \\ 0 & -1/\gamma \end{bmatrix} \begin{Bmatrix} \underline{i}_w \\ \underline{U}_w \end{Bmatrix}, \tag{8.55b}$$

where γ is the transducer constant, dependent on the distance d, the strength of the magnetic field and the geometry.

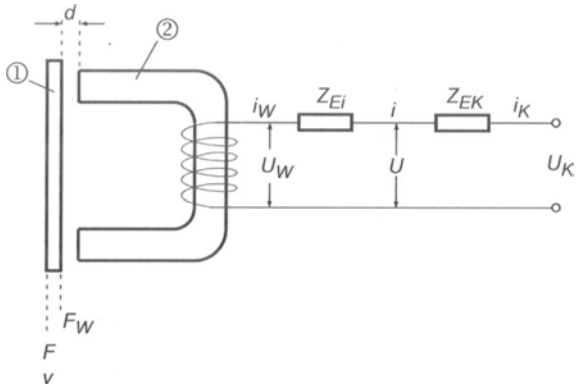

Fig. 8.29. Principle configuration of an electro-magnetic transducer. Ferro-magnetic armature (1) and permanent magnet (2)

A comparison with Eq. (8.40c) shows that save the numerical values, the transducer relations equal those of ideal electro-dynamic transducers. Also the role of the inner electrical impedance is the same since it results in a voltage drop. In both cases, the inner impedance consists of an inductance L_i and a resistance. Regarding the inner mechanical impedance, there is a small difference. Similar to the electro-static transducer, there is an attraction force which depends on the distance between the magnet and the armature and thus on their relative motion. As before, this leads to a negative stiffness cf., (8.51e). This means that Eq. (8.42d), again, can be adopted albeit with Z_{Mi} replaced by

$$Z'_{Mi} = Z_{Mi} - \frac{s_E}{j\omega} = Z_{Mi} - \frac{\gamma^2}{j\omega L_i}. \tag{8.55c}$$

As seen, the pivotal quantity with respect to the reaction of an electrical element on the mechanical impedance is, as always, the square of the transducer constant.

By multiplying the matrices (8.41d), (8.55b) and (8.41a), the relation for the physical electromagnetic transducer with an immobile magnet is obtained as

$$\begin{Bmatrix} \underline{F} \\ \underline{v} \end{Bmatrix} = \begin{bmatrix} \left(\gamma^2 + Z'_{Mi} Z_{Ei}\right)/\gamma & -Z'_{Mi}/\gamma \\ Z_{Ei}/\gamma & -1/\gamma \end{bmatrix} \begin{Bmatrix} \underline{i} \\ \underline{U} \end{Bmatrix}. \tag{8.55d}$$

From this relation, all the quantities of interest can be developed. If the motion of the magnet must be taken into account, the procedure demonstrated in Sect. 8.3.1.2 applies.

Electro-magnetic as electro-static transducers essentially are employed in the laboratory. Their advantage is that they are only weakly coupled to the test object and realize hardly any loading, also allowing for investigations of very light-weight systems.

8.3.5 Magnetostrictive Transducers

A magnetostrictive transducer most often consists of a rod of magnetostrictive material inserted in a coil as illustrated in Fig. 8.30. The primary magnetostrictive materials are nickel, some ferrites and, more recently, special alloys termed "giant magnetostrictive alloys" [8.10].

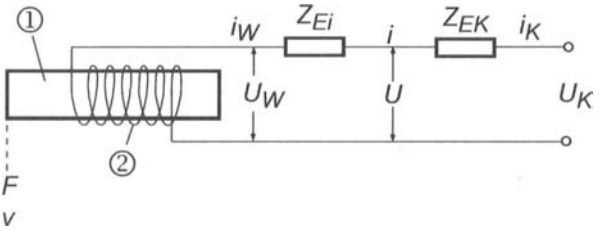

Fig. 8.30. Principle configuration of a magnetostrictive transducer. Magnetostrictive rod (1) and coil (2)

By passing a current i through the coil, the magnetic forces in the magnetostrictive material either shorten or lengthen the rod and constraining the rod at its ends results in a relatively large force. As stated previously, the force is proportional to the square of the magnetic flux. To achieve an alternating force, proportional to some supplied alternating current, a dc component is again required, such that the total and the transducer forces can be written as

$$\begin{aligned} F \propto \Phi^2 &= \frac{1}{2}\gamma_S i^2 = \frac{1}{2}\gamma_S(\bar{i}+\tilde{i})^2 \approx \frac{1}{2}\gamma_S \bar{i}^2 + \gamma_S \bar{i}\tilde{i}\,, \\ \underline{F}_w &= \gamma_S \bar{i}\,\underline{i}_w\,. \end{aligned} \tag{8.56a}$$

Since the transducer is reciprocal for $\bar{i} >> \tilde{i}$, an alternating voltage arises when the magnetostrictive transducer is compressed with the velocity v_w, which is given by

$$\underline{U}_w = -\gamma_S \bar{i}\,\underline{v}_w. \tag{8.56b}$$

With the exception of the altered symbols, these relations are the same as those for the electro-magnetic transducers. Moreover, since the effects of inner electrical and mechanical impedances are the same, the formulae of the previous section can be directly adopted.

Magnetostrictive transducers essentially are used in underwater acoustics. The attainable displacement amplitudes are very small. For nickel, the maximum relative elongation is of the order of 10^{-6} and for the giant magnetostrictive alloys 10^{-4} to 10^{-3}.

Despite the very simple design, the magnetostrictive transducers are only employed for special structure-borne sound problems [8.11]. Typically, there is a use when large force and small displacements are required such as at high frequencies. A disadvantage is the direct current required which is accompanied by resistive losses.

8.3.6 Elaboration on Reciprocal Transducers

8.3.6.1 M- *and* N-*Transducers*

By summarizing the transducer expressions for immobile magnets and backing electrodes respectively, those dependent on magnetic fields in (8.41f) and (8.55c) are described by

$$\begin{Bmatrix} \underline{F} \\ \underline{v} \end{Bmatrix} = \frac{1}{Bl_L} \begin{bmatrix} (Bl_L)^2 + Z_{Mi} Z_{Ei} & -Z_{Mi} \\ Z_{Ei} & -1 \end{bmatrix} \begin{Bmatrix} \underline{i} \\ \underline{U} \end{Bmatrix},$$
$$\begin{Bmatrix} \underline{F} \\ \underline{v} \end{Bmatrix} = \frac{1}{\gamma} \begin{bmatrix} \gamma^2 + Z'_{Mi} Z_{Ei} & -Z'_{Mi} \\ Z_{Ei} & -1 \end{bmatrix} \begin{Bmatrix} \underline{i} \\ \underline{U} \end{Bmatrix}, \tag{8.57a}$$

for the electro-dynamic and electro-magnetic as well as magnetostrictive transducers respectively. When all displacements are blocked, the force is proportional to the alternating current for this class of transducers.

For the transducers dependent on electro-static forces, (8.48), (8.49), (8.41a) and (8.52a) apply. One finds

$$\begin{Bmatrix} \underline{F} \\ \underline{v} \end{Bmatrix} = \frac{1}{K} \begin{bmatrix} -Z_{Mi} & K^2 + Z_{Mi}/Z_{Ei} \\ -1 & 1/Z_{Ei} \end{bmatrix} \begin{Bmatrix} \underline{i} \\ \underline{U} \end{Bmatrix},$$
$$\begin{Bmatrix} \underline{F} \\ \underline{v} \end{Bmatrix} = \frac{1}{\alpha} \begin{bmatrix} Z'_{Mi} & \alpha^2 + Z_{Mi}/Z_{Ei} \\ -1 & 1/Z_{Ei} \end{bmatrix} \begin{Bmatrix} \underline{i} \\ \underline{U} \end{Bmatrix}, \tag{8.57b}$$

for the piezo-electric and electro-static transducers. For this class of transducers, the forces are proportional to the alternating voltage as the displacements vanish.

Two of the relations in (8.57a) and (8.57b) still contains the flaw that the electrically induced, negative stiffness must be considered in the inner mechanical impedance Z'_{Mi}. By substituting (8.51f) and (8.55c) in (8.57b) and (8.57a) respectively, the electro-static description becomes

$$\begin{Bmatrix} \underline{F} \\ \underline{v} \end{Bmatrix} = \frac{1}{\alpha Z_{Ei}} \begin{bmatrix} (\alpha Z_{Ei})^2 + Z_{Mi} Z_{Ei} & Z_{Mi} \\ -Z_{Mi} & 1 \end{bmatrix} \begin{Bmatrix} \underline{i} \\ \underline{U} \end{Bmatrix}. \tag{8.57c}$$

Upon letting $Bl_L \to \alpha Z_{Ei}$, (8.57c) but the sign becomes identical to the formula for the electro-dynamic transducer. The electro-static and electro-dynamic transducers are categorized as *M*-transducers (equivalent voltage source). The description in (8.57c), moreover, would have been established directly from Eq. (8.54c), developed from Hamilton's principle.

In a similar way, one obtains

$$\begin{Bmatrix} \underline{F} \\ \underline{v} \end{Bmatrix} = \frac{1}{\gamma} \begin{bmatrix} Z_{Mi} & \gamma^2 + Z_{Mi}/Z_{Ei} \\ 1 & -1/Z_{Ei} \end{bmatrix} \begin{Bmatrix} \underline{i} \\ \underline{U} \end{Bmatrix}, \tag{8.57d}$$

for the electro-magnetic and magnetostrictive transducers from (8.57a) with (8.55c). Aside for the sign, this is also valid for the piezo-electric transducer. The latter electromagnetic and the magnetostrictive transducers are categorized as *N*-transducers (equivalent current source). Ultimately, however, the categorization is of a formal nature.

8.3.6.2 Reciprocity Calibration

The reciprocity of reciprocal transducers can be used also to calibrate electro-mechanical transducers without absolute measurements of dynamic quantities. The procedure is illustrated in two steps in Fig. 8.31 [8.12].

In the first step, a mass is given a velocity v_1 by means of an auxiliary exciter. Instead of a mass, any other mechanical structure can be used provided its impedance is well defined. The voltage proportional to the velocity is measured at the transducer *W* to be calibrated and the reciprocal transducer *R*,

$$\underline{U}_{W1} = \alpha_W \underline{v}_1 \,, \; \underline{U}_{R1} = \alpha_R \underline{v}_1. \tag{8.58a}$$

For the second step, the auxiliary exciter is turned off and the mass driven by the reciprocal transducer. The force F_2 and velocity v_2 resulting for a current i_{R2} are related by

$$\left|\underline{v}_2\right| = \left|\underline{F}_2 / Z\right| = \left|\alpha_R \underline{i}_{R2} / Z\right|, \tag{8.58b}$$

where *Z* is the known impedance. In this relation is used that the reciprocity principle or the law of mutual energies are valid such that

$$\left|\frac{\underline{U}_{R1}}{\underline{v}_1}\right| = \left|\frac{\underline{F}_2}{\underline{i}_{R2}}\right|, \quad \underline{U}_{R1}\underline{i}_{R2} = \underline{F}_2\underline{v}_1, \tag{8.58c}$$

respectively. Since the transducer to be calibrated should be linear, the voltage offered is

$$\underline{U}_{W2} = \alpha_W \underline{v}_2. \tag{8.58d}$$

By substitution of (8.58a) and (8.58b), v_2, α_R and v_1 can be eliminated and

$$|\alpha_W|^2 = \left|\frac{\underline{U}_{W1}\underline{U}_{W2}}{\underline{U}_{R1}\underline{i}_{R2}} Z\right|. \tag{8.58e}$$

Thus, the determination of the calibration factor α_W sought is transferred to measurements of electrical voltages and currents besides the knowledge of a well-defined impedance.

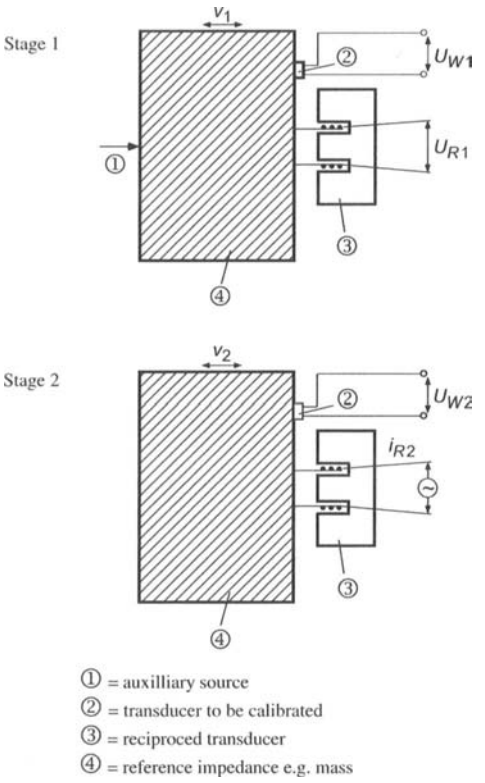

Fig. 8.31. Measurement of combined quantities associated with bending motion

Precise measurements of currents and voltages are usually straightforward as long as the reciprocal transducer is sufficiently strong to achieve a measurable signal over the entire range of interest. A well-defined impedance can be more cumbersome, however, since also for compact masses, the suspension may lead to deviations from the basic $Z = j\omega m$. Additionally, it must be taken into account that for small masses, all connected electrical equipment can noticeable affect the impedance.

8.4 Combined Quantities

With the transducers hitherto described, the displacement, velocity, acceleration or strain can be measured directly. In addition to these primary measurement quantities, more and more often some further are required, which can be derived from the former. For bending motion, for example, the first and second derivatives, corresponding to the cross-sectional rotation and the curvature respectively can be of interest. Those derived quantities can be obtained from finite differences formed from the signals from two or three identical or carefully calibrated transducers, as illustrated in Fig. 8.32. In this it is important that the distance Δx, on the one hand, does not become too small but, on the other, not too big. In the former situation, signals are subtracted of almost the same magnitude with enhanced errors as a risk whereas, in the latter, the finite difference will not be a satisfactory approximation of the corresponding differential. A reasonable compromise is to set Δx somewhere between a twentieth and a tenth of the wavelength.

Without strain gauges, strain can be measured also by using two adjacent sensors and approximating the spatial derivative in e.g., (3.1) by a finite difference.

A substantial problem for the structure-borne sound measurement technique as a whole is the fact that with the exception of optical methods in transparent structures, there are no means to undertake measurements in the interior of a structure without causing serious disturbances of the vibration field. Accordingly, one is forced to extract the interior motion from the results of measurements on the surfaces. As long as the structure is thin i.e., its thickness typically less than a sixth of the governing wavelength, such an extraction is principally possible. In that case, it can be assumed that all quantities are linearly related. Nonetheless, such measurements can prove rather laborious when different wave types must be distinguished. In Fig. 8.33 is exemplified the extraction of displacement, rotation, strain and cross-sectional contraction from measurements of eight displacement

quantities on two sides of a thin structure. Fortunately, such extensive and error prone measurements are only necessary on rare occasions since frequently, the most dominant component of motion can be identified and a proper transducer configuration devised.

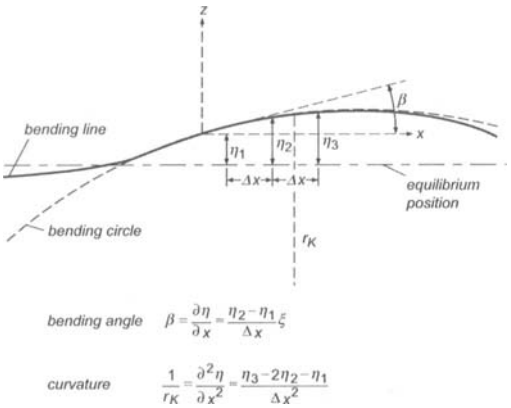

Fig. 8.32. Estimation of different components of motion from surface measurements

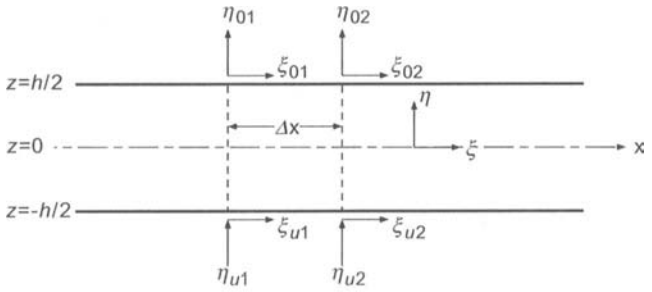

Bending displacement and bending angle at neutral layer

$$\eta = (\eta_u + \eta_0)/2 \quad , \quad \beta = \frac{\partial \eta}{\partial x} \approx \frac{(\eta_{u2} + \eta_{02}) - (\eta_{u1} + \eta_{01})}{2\Delta x}$$

In-plane displacement and strain in x-direction at neutral layer

$$\xi = (\xi_u + \xi_0)/2 \quad , \quad \frac{\partial \xi}{\partial x} \approx \frac{(\xi_{u2} + \xi_{02}) - (\xi_{u1} + \xi_{01})}{2\Delta x}$$

Cross-sectional contraction at surfaces

$$\varepsilon_Z = (\eta_0 + \eta_u)/h$$

Fig. 8.33. Determination of various motion components from measurements on the surfaces of a plate or shell structure

In conjunction with measurements of structure-borne sound intensity, registration of stress and velocity is required as indicated by the expression in Sect. 3.9. Again, the velocity registration is comparatively straightforward, at least a far as the necessary quantities representing the interior motion can be deduced from measurements at the surfaces. In contrast, the determination of stresses is more intricate from two aspects [3.27,3.28]:

- The stress-strain relations comprise several strain components cf., (3.119) and (3.162a), such that a set of finite differences would have to be formed. Due to the complicated and error prone finite difference operators, simple states of deformation are assumed, for which simple stress-strain relations are available, (3.2), (3.42), (3.54), (3.73) and (3.223f).
- The stresses can be calculated from the strains only when some properties such as Young's modulus or shear modulus are known for the material at the measurement position. This means that certain knowledge must be present in advance.

At present, measurement of structure-borne sound intensity in slender rods and beams as well as in thin plates and shells is practicable in the laboratory. The employment of the technique in everyday practice will probably take a while although the insight gain from knowledge of the intensities and power transmissions would be of great help in many practical applications.

References

[8.1] Bragg W., 1929. An instrument for measuring small amplitudes of vibrations. Journal of Scientific Instruments, 6, p. 196
[8.2] Cremer L. and Klotter K., 1959. Neuer Blick auf die elektrisch-mechanischen Analogien. Ingenieur-Archiv, 28, p. 27
[8.3] Halliwell N.A., 1979. Laser-doppler measurement of vibrating surfaces: A portable instrument. Journal of Sound and Vibration, 62, p. 312
[8.4] Neubert H., 1975. Instrument transducers: An introduction to their performance and design. Clarendon Press, Oxford
[8.5] Lenk A., 1977. Elektromechanische Systeme, Band 1,2. VEB Verlag, Berlin
[8.6] Harris C.M. and Crede C.E., 1976. Shock and vibration handbook, Ch. 13-22. McGraw-Hill
[8.7] Crawley E.F. and de Luis J., 1987. Use of piezoelectric actuators as elements of intelligent structures. AIAA Journal, 25, p. 1373
[8.8] Hertz H., 1884. Die Principien der Mechanik in neuem Zusammenhang dargestellt. Drei Arbeiten von Heinrich Hertz mit einem Vorwort von H.von Helmholtz. Akademische Verlagsanstalt, Leipzig

[8.9] Meyer E. and Guicking D., 1974. Schwingungslehre Ch. 3. Vieweg, Braunschweig
[8.10] Savage H.T., Abbundi R., Clark A.E. and McMasters O.D., 1979. Permeability, magnetomechanical coupling and magnetostriction in grain-oriented rare earth-iron alloys. Journal of Applied Physics, 50, B3, p. 1674
[8.11] Petersson B.A.T., 1987. On the use of giant magnetostrictive devices for moment excitation. Journal of Sound and Vibration, 116, p. 191
[8.12] Beranek L.L., 1954. Acoustics, part XXIX. McGraw-Hill, New York NY